

1986

# Electrochemical Studies of Transition Metal Carbonyls

Dwayne Edward Cooper

*Eastern Illinois University*

This research is a product of the graduate program in [Chemistry](#) at Eastern Illinois University. [Find out more](#) about the program.

---

## Recommended Citation

Cooper, Dwayne Edward, "Electrochemical Studies of Transition Metal Carbonyls" (1986). *Masters Theses*. 2637.  
<https://thekeep.eiu.edu/theses/2637>

This is brought to you for free and open access by the Student Theses & Publications at The Keep. It has been accepted for inclusion in Masters Theses by an authorized administrator of The Keep. For more information, please contact [tabruns@eiu.edu](mailto:tabruns@eiu.edu).

# THESIS REPRODUCTION CERTIFICATE

TO: Graduate Degree Candidates who have written formal theses.

SUBJECT: Permission to reproduce theses.

The University Library is receiving a number of requests from other institutions asking permission to reproduce dissertations for inclusion in their library holdings. Although no copyright laws are involved, we feel that professional courtesy demands that permission be obtained from the author before we allow theses to be copied.

Please sign one of the following statements:

Booth Library of Eastern Illinois University has my permission to lend my thesis to a reputable college or university for the purpose of copying it for inclusion in that institution's library or research holdings.

8-8-86

Date

Author

I respectfully request Booth Library of Eastern Illinois University not allow my thesis be reproduced because \_\_\_\_\_

Date

Author

**Electrochemical Studies**

---

**of Transition Metal Carbonyls**

---

(TITLE)

BY

**Dwayne Edward Cooper**

**THESIS**

SUBMITTED IN PARTIAL FULFILLMENT OF THE REQUIREMENTS  
FOR THE DEGREE OF

**Master of Science in Chemistry**

---

IN THE GRADUATE SCHOOL, EASTERN ILLINOIS UNIVERSITY  
CHARLESTON, ILLINOIS

**1986**

---

YEAR

I HEREBY RECOMMEND THIS THESIS BE ACCEPTED AS FULFILLING  
THIS PART OF THE GRADUATE DEGREE CITED ABOVE

8/20/86  
DATE

8/20/86  
DATE

**Electrochemical Studies of Transition Metal Carbonyls**

**by**

**Dwayne E. Cooper  
B.S. in Chemistry, May, 1982  
Eastern Illinois University  
Charleston, Illinois**

**Submitted in partial fulfillment  
of the requirements for the degree of  
Master of Science in Chemistry at the  
Graduate School of Eastern Illinois University  
Charleston, Illinois  
1986**

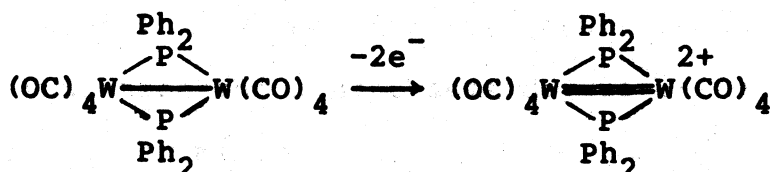
## ABSTRACT

The electrochemical oxidation of  $(OC)_5MP-PM'(CO)_5$  ( $M=Cr, Mo, W$ ;  $M'=Cr, Mo, W$ ;  $M=M'$  or  $M \neq M'$ ;  $P-P=Ph_2PCH_2CH_2PPh_2$ ) and the reduction of the oxidized products in a 0.1 M tetrabutylammonium perchlorate methylene chloride solution at a platinum disc working electrode with a Ag/AgCl reference electrode have been studied. The number of electrons in the oxidation step was determined by comparison with the one electron oxidation of ferrocene which had a peak potential at +0.15 V.

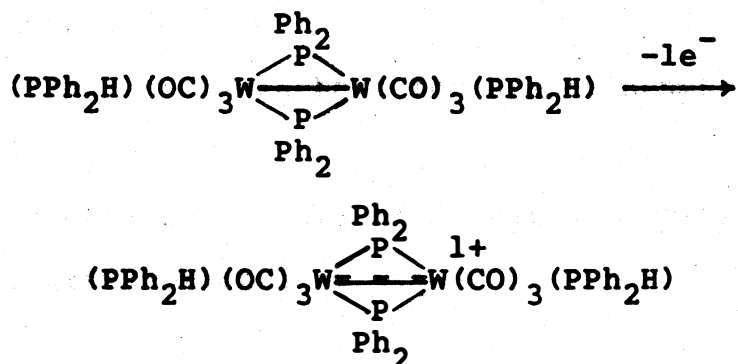
The cyclic voltammograms of the homobimetallic and heterobimetallic complexes display two general characteristics: quasi-reversible or irreversible one electron oxidation of each individual metal center. The chromium-chromium complex exhibits two oxidation peaks with peak potentials at +1.04 V and +1.35 V. The first oxidation peak coupled with a cathodic peak exhibits quasi-reversible behavior while the second oxidation peak exhibits irreversible behavior. The molybdenum and tungsten homobimetallic species each possess an irreversible oxidation peak at 1.06 V and 1.12 V, respectively. The heterobimetallics all exhibit irreversible behavior. The voltammograms have a single oxidation peak without a coupled cathodic peak. The anodic peak potentials occur at +0.94, +0.96, and +1.05 volts for the chromium-molybdenum, chromium-tungsten, and molybdenum-tungsten complex, respectively.

Cyclic voltammograms were also obtained for  $(OC)_4W(Ph_2P)_2W(CO)_4$  (III) and  $HPh_2P(OC)_3W(Ph_2P)_2W(CO)_3PPh_2H$

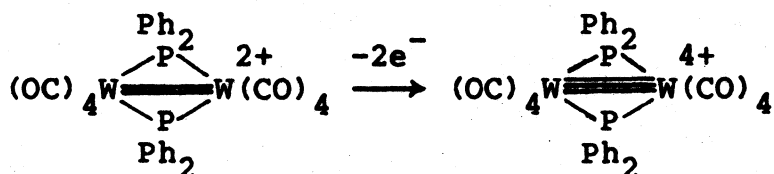
(IV). The first oxidation step was coupled to a cathodic peak for each of the phosphido-bridged complexes. The peak to peak separations and peak ratios exhibit reversible behavior. The anodic peak potential for (III), corresponding to a two electron change, occurs at +0.75 V.



For complex (IV) the anodic peak potential, corresponding to a one electron change, was found at +0.19 V.



Complexes (III) and (IV) undergo second oxidation steps which are irreversible as shown by the absence of a cathodic peak. For complex (III), the second anodic peak potential was found at +1.02 V with a peak height equal to two electrons.



Complex (IV) loses a second electron at +0.72 V and a third electron at +1.4 V, accompanied by formation of metal-metal bonds of bond order 2 and 2 1/2, respectively.

## ACKNOWLEDGEMENTS

I would sincerely like to thank my wife Therese for all her loving support during this project. The strong friendship and happiness she provided made this goal possible and many more to look forward to.

I am grateful to my mom for her encouragement throughout my college education and I hope some day to bring up a son as well as she brought me up.

Thank you E. I. U. Chemistry Department for the fine education. Special thanks to my advisor Dr. Sherman and my backup advisor Dr. Keiter. Thanks Ken and Matt for the pleasant conversation.

I must thank Mr. Rhinehart for his guidance at an important time.

I appreciate the efforts of my personal secretary Jill and personal artist Michelle.

# TABLE of CONTENTS

	page
I. INTRODUCTION.....	1
II. EXPERIMENT L.....	10
1. Equipment and Electrochemical Cell.....	10
A. Fume Hood.....	10
B. Electrochemical Cell.....	10
C. Electrodes.....	12
1. Working Electrode (DME).....	12
2. Working Electrode (Pt Disc).....	12
3. Reference Electrode.....	13
4. Auxiliary Electrode.....	14
D. Reagents.....	14
1. Mercury.....	15
2. Supporting Electrolyte.....	15
3. Methylene Chloride.....	16
4. Nitrogen.....	17
E. Equipment.....	18
F. Typical Procedure for Current-Voltage Curves.....	18
III. RESULTS and DISCUSSION.....	20
1. Ferrocene as an Internal Standard.....	20
A. Cyclic Voltammetry of Ferrocene.....	20
B. Polarography of Ferrocene.....	26
2. Cyclic Voltammetry of Group VI Metal Carbonyls.....	33
A. Homobimetallic Complexes.....	33
1. $(OC)_5CrPPh_2CH_2CH_2Ph_2PCr(CO)_5$ .....	33
A. $^5$ Addition of $^2$ Excess Ligand $Ph_2P$ .....	37
2. $(OC)_5MoPPh_2CH_2CH_2Ph_2PMo(CO)_5$ .....	44
3. $(OC)_5WPPh_2CH_2CH_2Ph_2PW(CO)_5$ .....	47
B. Heterobimetallic Complexes.....	52
1. $(OC)_5CrPPh_2CH_2CH_2Ph_2PMo(CO)_5$ .....	52
2. $(OC)_5CrPPh_2CH_2CH_2Ph_2PW(CO)_5$ .....	55
3. $(OC)_5MoPPh_2CH_2CH_2Ph_2PW(CO)_5$ .....	58
C. Phosphido-Bridged Tungsten Carbonyls.....	61
1. $(OC)_4W(Ph_2P)_2W(CO)_4$ .....	61
2. $HPH_2P(OC)_3W(Ph_2P)_2W(CO)_3PPh_2H$ .....	67
B. $^2$ Polarography of $HPH_2P(OC)_3W(Ph_2P)_2W(CO)_3PPh_2H$ .....	76
IV. CONCLUSIONS.....	82
LITERATURE CITED.....	85
VITA.....	88



# LIST of FIGURES

figure	page
1. Voltammogram of $6.0 \times 10^{-4}$ M ferrocene in a 0.10 M TBAP-methylene chloride solution (1.0 V/min.).....	22
2. Diffusion control plot of ferrocene.....	28
3. Plot of EQUATION 5. Reversibility, n and $E_{1/2}$ determination of ferrocene.....	31
4. Voltammogram of $5.47 \times 10^{-4}$ M (OC) <sub>5</sub> CrPPh <sub>2</sub> CH <sub>2</sub> CH <sub>2</sub> Ph <sub>2</sub> PCr(CO) <sub>5</sub> in a 0.10 M TBAP-methylene chloride solution (5.0 V/min.).....	34
5. Voltammogram of $4.80 \times 10^{-4}$ M (OC) <sub>5</sub> CrPPh <sub>2</sub> CH <sub>2</sub> CH <sub>2</sub> Ph <sub>2</sub> PCr(CO) <sub>5</sub> and $1.00 \times 10^{-3}$ M Ph <sub>3</sub> P in a 0.10 M TBAP-methylene chloride solution.....	38
6. Voltammogram of $5.62 \times 10^{-4}$ M (OC) <sub>5</sub> CrPPh <sub>2</sub> CH <sub>2</sub> CH <sub>2</sub> Ph <sub>2</sub> PCr(CO) <sub>5</sub> and $9.94 \times 10^{-2}$ M Ph <sub>3</sub> P in a 0.10 M TBAP-methylene chloride solution.....	41
7. Voltammogram of $4.73 \times 10^{-4}$ M (OC) <sub>5</sub> MoPPh <sub>2</sub> CH <sub>2</sub> CH <sub>2</sub> Ph <sub>2</sub> PMo(CO) <sub>5</sub> in a 0.10 M TBAP-methylene chloride solution (5.0 V/min.).....	45
8. Voltammogram of $4.44 \times 10^{-4}$ M (OC) <sub>5</sub> WPPPh <sub>2</sub> CH <sub>2</sub> CH <sub>2</sub> Ph <sub>2</sub> PW(CO) <sub>5</sub> in a 0.10 M TBAP-methylene chloride solution (5.0 V/min.).....	50
9. Voltammogram of $5.18 \times 10^{-4}$ M (OC) <sub>5</sub> CrPPh <sub>2</sub> CH <sub>2</sub> CH <sub>2</sub> Ph <sub>2</sub> PMo(CO) <sub>5</sub> in a 0.10 M TBAP-methylene chloride solution (2.0 V/min.).....	53
10. Voltammogram of $4.30 \times 10^{-4}$ M (OC) <sub>5</sub> CrPPh <sub>2</sub> CH <sub>2</sub> CH <sub>2</sub> Ph <sub>2</sub> PW(CO) <sub>5</sub> in a 0.10 M TBAP-methylene chloride solution (2.0 V/min.).....	56
11. Voltammogram of $4.93 \times 10^{-4}$ M (OC) <sub>5</sub> MoPPh <sub>2</sub> CH <sub>2</sub> CH <sub>2</sub> Ph <sub>2</sub> PW(CO) <sub>5</sub> in a 0.10 M TBAP-methylene chloride solution (10.0 V/min.).....	59
12. Voltammogram (first peak) of $3.68 \times 10^{-4}$ M (OC) <sub>4</sub> W(PPh <sub>2</sub> ) <sub>2</sub> W(CO) <sub>4</sub> in a 0.10 M TBAP-methylene chloride solution (2.0 V/min.).....	63
13. Voltammogram (first and second peak) of $3.68 \times 10^{-4}$ M (OC) <sub>4</sub> W(PPh <sub>2</sub> ) <sub>2</sub> W(CO) <sub>4</sub> in a 0.10 M TBAP-methylene chloride solution (1.0 V/min.).....	65
14. Voltammogram (first peak) of $3.22 \times 10^{-4}$ M HPh <sub>2</sub> P(OC) <sub>3</sub> W(PPh <sub>2</sub> ) <sub>2</sub> W(CO) <sub>3</sub> PPh <sub>2</sub> H in a 0.10 M TBAP-methylene chloride solution (2.0 V/min.).....	68
15. Voltammogram (first and second peak) of $3.22 \times 10^{-4}$ M HPh <sub>2</sub> P(OC) <sub>3</sub> W(PPh <sub>2</sub> ) <sub>2</sub> W(CO) <sub>3</sub> PPh <sub>2</sub> H in a 0.10 M TBAP-methylene chloride solution (2.0 V/min.).....	71
16. Voltammogram (1 <sup>st</sup> , 2 <sup>nd</sup> and 3 <sup>rd</sup> peak) of $3.22 \times 10^{-4}$ M HPh <sub>2</sub> P(OC) <sub>3</sub> W(PPh <sub>2</sub> ) <sub>2</sub> W(CO) <sub>3</sub> PPh <sub>2</sub> H in a 0.10 M TBAP-methylene chloride solution (2.0 V/min.).....	74

# LIST of FIGURES

Figure	Page
17. Polarogram of $3.22 \times 10^{-4}$ M $\text{HPh}_2\text{P}(\text{OC})_3\text{W}(\text{PPh}_2)_2\text{W}(\text{CO})_3\text{PPh}_2\text{H}$ in a 0.10 M TBAP- methylene chloride solution.....	77
18. Plot of EQUATION 5. Reversibility, n and $E_{1/2}$ determination of $\text{HPh}_2\text{P}(\text{OC})_3\text{W}(\text{Ph}_2\text{P})_2\text{W}(\text{CO})_3\text{PPh}_2\text{H}$ ....	80

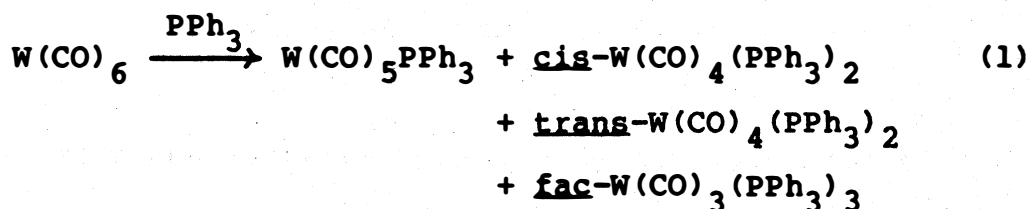
# LIST of TABLES

tables	page
1. Cyclic Voltammetry Data of Ferrocene.....	26
2. Polarography Data of Ferrocene for the Plot of LOG( $i_L$ ) versus LOG( $h_{corr}$ ).....	27
3. Polarography Data of Ferrocene for the Plot of $E_{DME}$ versus LOG( $i/i_d - i$ ).....	30
4. Cyclic Voltammetry Data of (OC) <sub>5</sub> CrPPh <sub>2</sub> CH <sub>2</sub> CH <sub>2</sub> Ph <sub>2</sub> PCr(CO) <sub>5</sub> .....	37
5. Cyclic Voltammetry Data of HPh <sub>2</sub> P(OC) <sub>3</sub> W(Ph <sub>2</sub> P) <sub>2</sub> W(CO) <sub>3</sub> PPh <sub>2</sub> H.....	70
6. Polarographic Data of HPh <sub>2</sub> P(OC) <sub>3</sub> W(Ph <sub>2</sub> P) <sub>2</sub> W(CO) <sub>3</sub> PPh <sub>2</sub> H for the Plot of $E_{DME}$ versus LOG( $i/i_d - i$ ).....	79

## I. INTRODUCTION

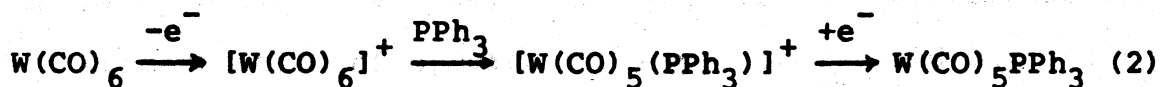
Electrochemistry is a surface science. This is in contrast to most methods of chemical measurement which involve homogeneous solutions. Electrochemical studies of inorganic and organometallic complexes of the transition metals have become increasingly popular. This is especially true in the case of cyclic voltammetry, a technique which is ideal for routine characterization of redox properties of new molecules. [1] The chemical reversibility of many electrochemical reactions and the accessibility of reduced or oxidized states determined by cyclic voltammetry has led to the development of new electrochemical synthetic methods. [2]

Traditionally, substitution reactions of metal carbonyl complexes have been carried out under thermal or photochemical conditions. For example, the photochemical reaction of  $\text{W(CO)}_6$  with  $\text{PPh}_3$  gives rise to a mixture of products all of which are formed in poor yield (EQUATION 1).



The use of electrodes as "reagents" may allow for the electrochemical displacement of CO from a metal carbonyl complex in a manner much more specific than that observed with photochemical or thermal techniques. When  $\text{W(CO)}_6$  is oxidized to the 17-electron complex,  $[\text{W(CO)}_6]^+$ , carbon monoxide is

readily displaced by a tertiary phosphine. The substituted derivative finds an electron to form the neutral product (EQUATION 2).



A heterogeneous electrochemical reaction can take place only at the interface between the electrode and the solution of electrolyte. The electrode can affect or sense only that part of the solution which is in immediate contact with it. For example, ferrocene can not be oxidized if it is absent at the interface, even if ferrocene exists elsewhere in the cell. Therefore, the properties of the electrode-solution interface and the form of mass transport should be considered.

The rate,  $v$ , at which the electroactive species is brought to the electrode surface by mass transport is directly proportional to faradaic current (EQUATION 3). [3]

$$v(\text{mol sec}^{-1} \text{ cm}^{-2}) = i/nFA \quad (3)$$

where  $i$ =current (amperes),  $F$ =faraday (coulombs/mol of electrons),  $A$ =area( $\text{cm}^2$ ),  $n$ =mol electron/mol electro-active specie.

The Nernst-Planck equation describes mass transfer to an electrode for a one-dimensional system (EQUATION 4). [4]

$$J_i(x) = -D_i \partial C_i(x) / \partial x - (Z_i F / RT) D_i C_i \partial \phi(x) / \partial x + C_i v(x) \quad (4)$$

$J_i(x)$  is the flux of species  $i$  ( $\text{mol sec}^{-1} \text{ cm}^{-2}$ ) at distance  $x$  from the surface,  $D_i$  is the diffusion coefficient ( $\text{cm}^2/\text{sec}$ ),  $\partial C_i(x)/\partial x$  is the concentration gradient at distance  $x$ ,  $\partial \phi/\partial x$  is the potential gradient,  $z_i$  and  $C_i$  are the charge number and concentration of species  $i$ , respectively, and  $v(x)$  is the velocity ( $\text{cm/sec}$ ) with which a volume element in solution moves along the axis. There are three types of mass transport that can occur and are represented by the three terms on the right side of the equation. The first term is diffusion, which is the movement of a species because of a concentration gradient. Migration, the second term, is the movement of a charged species in an electric field. The third term is convection or stirring. To simplify the experiment, the electrochemical system is designed to allow only one mode of mass transport. An ionic electrolyte is added in large concentration relative to the analyte to suppress migration and, measurements are made with the electrochemical cell at quiescent conditions. Therefore, the mode of mass transport in this study is solely by diffusion. Since the current is proportional to the concentration of the electroactive species and electrode area, the relationship between the mode of mass transport, diffusion, and rate of electrode reaction can be expressed (EQUATION 5).

$$J_i(x=0) = -D_i(\partial C_i/\partial x)_{x=0} = i/nFA \quad (5)$$

The depletion of reactants at the electrode surface during

oxidation causes a concentration gradient to develop. The concentration of the species in the vicinity of the electrode,  $C^e$ , is then different from the concentration of the electroactive species in bulk of solution,  $C^b$  (EQUATION 6). [5]

$$i/nFA = D_i (C_i^b - C_i^e) \quad (6)$$

The electroactive species diffusing to the working electrode from the bulk of solution is fastest when its concentration at the electrode surface is zero. As the reaction proceeds at the electrode solution interface, more electroactive species diffuse into the depleted zone. The current which flows under these conditions is called the limiting or diffusion current (EQUATION 7). [6]

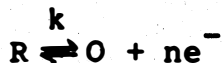
$$i_d = nFAD_i C_i^b \quad (7)$$

This is the maximum rate of current flow because the electroactive species is being oxidized or reduced as fast as it can be brought to the electrode surface. The concentration of the oxidized and reduced species at the electrode surface obeys the Nernst equation if the electron transfer is rapid and the system is chemically reversible (EQUATION 8). [7]

$$E = E^0 + (RT/nF) \ln [C_O^e / C_R^e] \quad (8)$$

It is very important to define the concept of chemical reversibility. Using EQUATION 9, some distinctions can be

made.



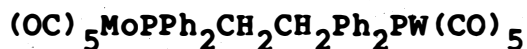
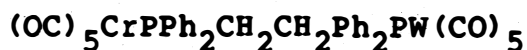
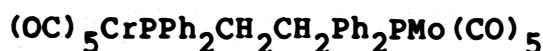
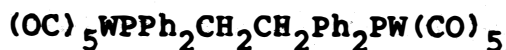
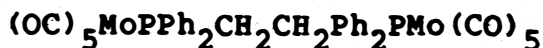
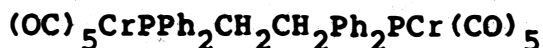
A rapid reversible or Nernstian electron transfer step implies that no structural changes occur between the oxidized form (O) and the reduced form (R), although the heterogeneous rate constant gives no information on the chemical stability of (O). [8] In this study, the primary concern is the generation and ultimate fate of the electrode product (O). Therefore, the factor which is most important is the chemical reversibility of the redox couple. This refers to the chemical stability of (O). A cell reaction is said to be chemically reversible when the forward half-reaction can be reversed by reversing the direction of current flow. The cell reaction is chemically irreversible if the reaction is not reversed when the direction of current flow is reversed. Using cyclic voltammetric techniques it is possible to show that the oxidation reduction couple of a reaction is chemically reversible or irreversible.

The electrochemical oxidation of neutral 18-electron group VI metal carbonyl complexes to give labile 17-electron radical cations is quite important considering that ligand substitution usually proceeds by even numbered electron intermediates. Typically one two-electron donor such as CO is displaced by another two-electron donor such as  $R_3P$  or  $R_2C=CR_2$ . This is the case for the industrially important hydroformylation process in which the 16-electron catalytic complex  $HCo(CO)_3$  is generated from the 18-electron complex,



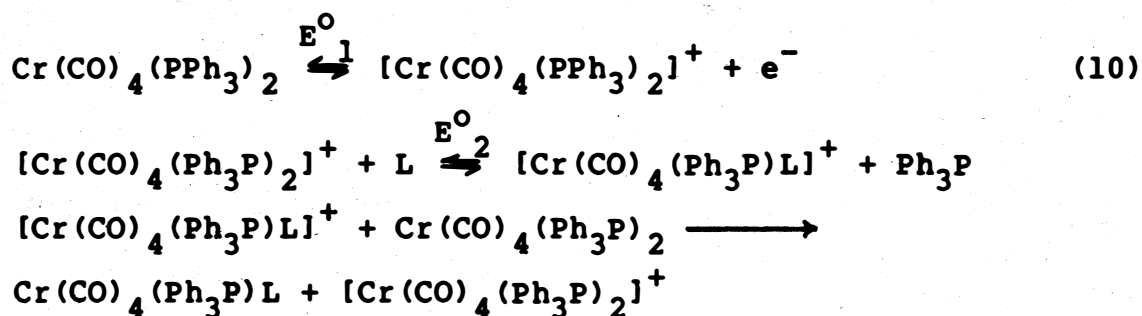
$\text{HCo}(\text{CO})_4$ . [9] The catalyst combines with  $\text{H}_2\text{C}=\text{CH}_2$  to give the 18-electron  $\text{HCo}(\text{CO})_3(\text{H}_2\text{C}=\text{CH}_2)$ .

The redox properties of a series of group VI complexes which exhibit 17-electron oxidation products, have been examined to learn more about their reactivity. Complexes of the following structure were studied:



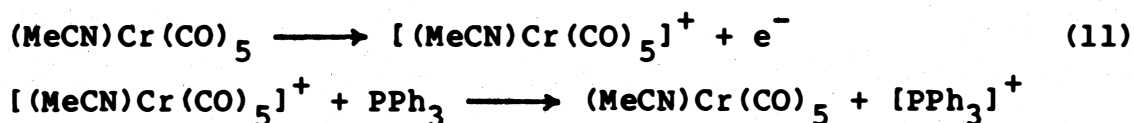
There have been several similar studies on the redox properties of related group VI carbonyl complexes. For example, the redox properties for a series of group VI complexes having the formula  $\text{M}(\text{CO})_5\text{L}$  where  $\text{L}=\text{PH}_3\text{P}$ ,  $\text{CH}_3\text{CN}$  or pyridine and  $\text{M} = \text{Cr}, \text{Mo}, \text{W}$  were shown to have a single electron transfer in the first oxidation step. [10] Electrochemical oxidation pathways have also been characterized for  $\text{M}(\text{CO})_2(\text{DPM})_2$  where  $\text{M} = \text{Cr}, \text{Mo}, \text{W}$  and  $\text{DPM} =$  bis(diphenylphosphino)methane. Stable 17-electron species were generated as well as 16-electron complexes. [11] It is evident from these studies that variations in ligand substitution and central metal are extremely important to thermodynamic and kinetic stabilities of the oxidized complexes.

Electron-transfer catalysis reactions initiated by ligand substitution reactions have been studied by others and were touched upon in this study. [12] The basis for catalysis is the oxidation of an 18-electron metal carbonyl producing a relatively reactive 17-electron species which acts as the catalyst. This species may react with the solvent or excess ligand to generate a new 17-electron species that can thermodynamically, at least, react with the starting material in a homogeneous redox reaction to give a new substituted 18-electron species and regenerate the catalyst (EQUATION 10).

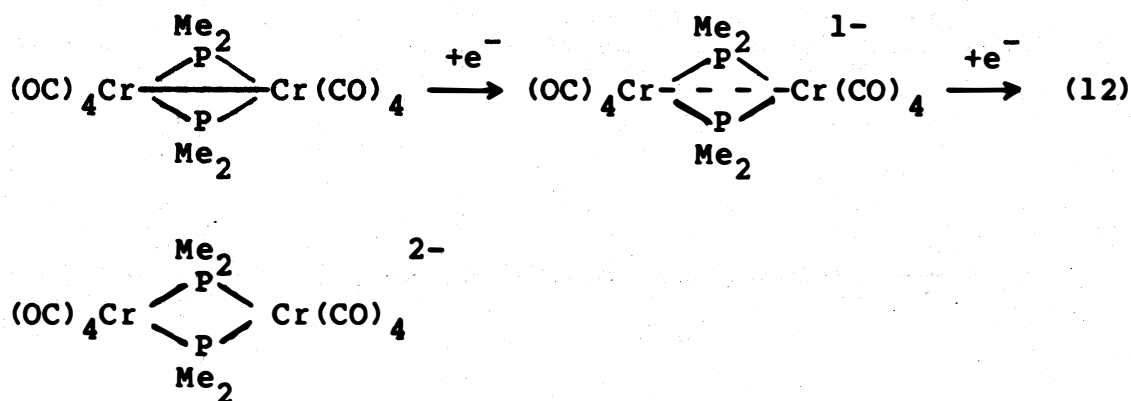


The thermodynamic requirement for this cycle to operate is that  $\text{E}^{\text{O}}_1$  be less positive than  $\text{E}^{\text{O}}_2$ .

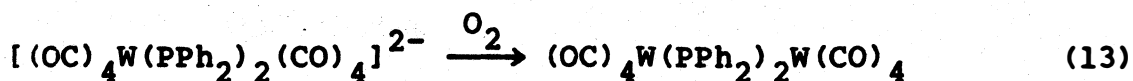
Kochi has found enhanced oxidation of  $\text{Ph}_3\text{P}$  catalyzed by metal carbonyls,  $(\text{py})\text{Cr(CO)}_5$  and  $(\text{MeCN})\text{Cr(CO)}_5$ . [13] The electrode process consists of a reversible charge transfer followed by chemical regeneration of the reduced species (EQUATION 11).



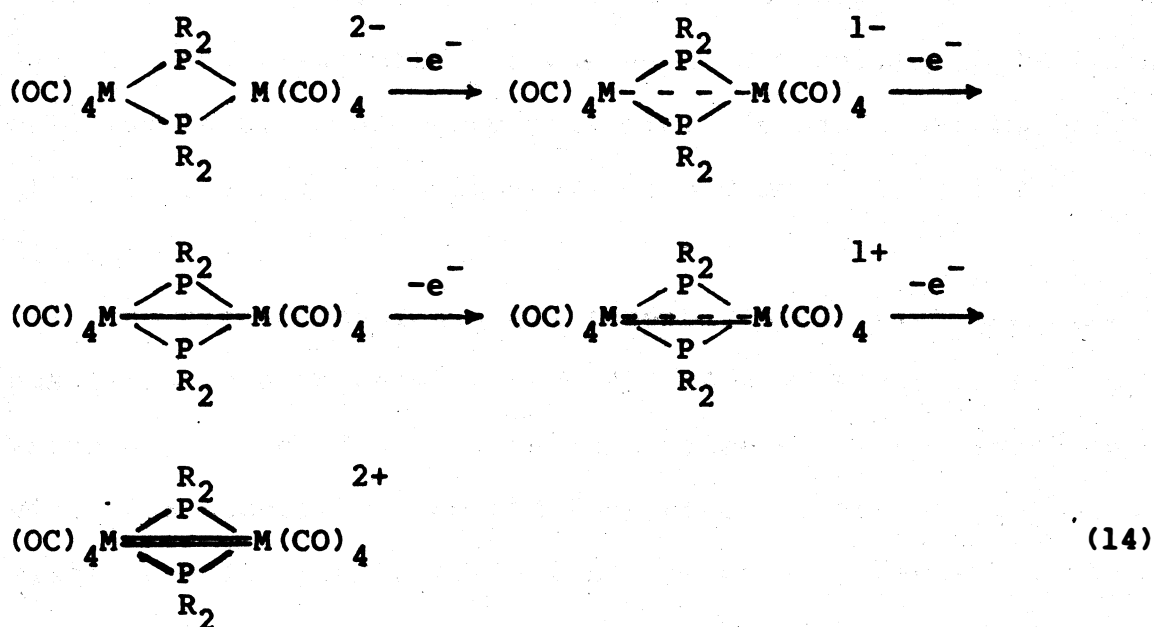
Our study also includes phosphido-bridged complexes which have the general formula,  $(OC)_3LW(PPh_2)_2WL(CO)_3$ , ( $L = CO$  or  $PPh_2H$ ). It was expected that these complexes would have interesting redox chemistry. Prior to this work, Dessy and others had shown that  $(OC)_4Cr(PMe_2)_2Cr(CO)_4$  can be reduced both chemically (metallic Na) and electrochemically. [14] Two electrons were added in a stepwise reduction (EQUATION 12).



The ESR spectrum was recorded for the monoanion, a species which has an odd number of electrons. The reduction corresponds to destruction of a Cr-Cr single bond to give first a Cr-Cr bond with bond order 1/2 and finally a bond order of zero. A similar dianion,  $[(OC)_4W(PPh_2)_2W(CO)_4]^{2-}$ , has been synthesized by the reduction of  $(OC)_4W(PPh_2)_2W(CO)_4$  with  $LiAlH_4$ . [15] These dianionic species are air sensitive and react with  $O_2$  to regenerate the neutral complex. (EQUATION 13).



No one has succeeded, however, in oxidizing  $(OC)_4M(PR_2)_2M(CO)_4$  to a stable cation. The possibility exists for the formation of a metal-metal bond with bond orders of 1 1/2 and 2. One could envision an electron change of 4 as one proceeds from  $[(OC)_4(PR_2)_2M(CO)_4]^{2-}$  to  $[(OC)_4M(PR_2)_2M(CO)_4]^{2+}$  (EQUATION 14).



The cationic complexes, if found, might be stabilized by some bulky anion such as  $BF_4^-$ ,  $PF_6^-$  or  $Ph_4B^-$ . Cationic organo-metallic complexes have been overlooked until recently. The synthesis of  $[Fe(CO)_3(PR_3)_2]^+$  and  $[Cr(CO)_5PR_3]^+$  are just two examples of recently synthesized cations, both of which were initially observed electrochemically. [16]

## II. EXPERIMENTAL

### 1. EQUIPMENT and ELECTROCHEMICAL CELL

The experimental equipment, all of which will be explained in detail in the following sections, consisted of potentiostat and programmer, X-Y recorder, oscilloscope and camera, electrochemical cell, and temperature bath.

#### A. FUME HOOD

The entire experimental setup was placed in a fume hood because methylene chloride was used as a solvent. Methylene chloride is toxic and very volatile. It has a boiling point of  $39.95^{\circ}\text{C}$  and a vapor pressure of 400 mm Hg @  $24.1^{\circ}\text{C}$ .

[17,18]

The electrochemical cell assembly along with the Pyrex gas lines were mounted on two 24"x 24"x 2" slabs of slate which were mounted on a tire inner tube so as to reduce any vibration occurring from the fume hood. Placed on top of the slate were 150 pounds of lead bricks to help dampen vibrations. An experimental check for vibrations (i.e. diffusion control) will be discussed in Section III. Data show that the vibrations do not affect the experiment in a time window of approximately twenty seconds, at which time the electron transfer is well over.

#### B. ELECTROCHEMICAL CELL

The electrochemical cell was used in both polarographic and cyclic voltammetric studies. In conventional polarography

and voltammetry problems result when the resistance due to nonaqueous solvents exceeds 500 ohms. The  $iR$  drop across this high resistance causes the potential between the polarized electrode and the reference electrode to differ from the applied potential. Furthermore, this potential error is not constant due to large changes in current during electrochemical measurements. Measuring this resistance and correcting for  $iR$  drop is a tedious process. The potentiostat eliminates this process by electronically controlling the potential of the polarized electrode and thus compensating for  $iR$  drop. A three-electrode system was used to reduce this resistance. The three electrodes were the working electrode (either a dropping mercury electrode (DME) or platinum disc electrode), a silver-silver ion reference electrode and a coiled platinum wire auxiliary electrode. The 100-mL Pyrex electrochemical cell (IBM Instruments), had a Teflon cap with five ports each fitted with Teflon sleeves. The working, reference, and auxiliary electrodes and two gas dispersion tubes were introduced through these ports. The cell was of air-tight design with high vacuum Teflon valves and O-ring seals to allow an inert atmosphere to be maintained without contamination by grease and also to prevent any evaporation of solution and to retain an inert atmosphere. The evaporation of the solution was a problem during lengthy experiments but was easily detected by the nonreproducibility of the peak currents. The cell was also threaded to accommodate a plastic jacketed water bath for controlling the solution

temperature.

## C. ELECTRODES

### 1. WORKING ELECTRODE (DME)

The working electrode for the polarographic studies was a dropping mercury electrode of conventional design. A short piece of securely fastened Tygon tubing was used to fasten the capillary to the standpipe assembly. The capillary (Sargent Welch) was 14.1 cm in length and filled with mercury by means of a 150-mL reservoir which was connected to the standpipe with Tygon tubing. Dilute nitric acid was used to clean the tip of the capillary. When not in use the capillary was stored in air. The mass flow rate of the capillary employed was determined by weighing the amount of mercury delivered from the capillary over a 25-drop interval. The mass flow rate was determined at open circuit potential. The capillary characteristics for the dropping mercury electrode are  $m = 1.660$  mg/sec and  $t = 122$  sec. From EQUATION 15 the area of a drop can be determined. [19] The area of a drop was found to be  $A = 0.034$  cm<sup>2</sup>.

$$A = 4\pi(3mt/4\pi d_{Hg})^{2/3} \quad (15)$$

### 2. WORKING ELECTRODE (Pt Disc)

The working electrode for the voltammetric studies was a planar platinum disc electrode (IBM Instruments) used in the stationary mode with a 0.203 cm<sup>2</sup> electrochemical area. The

development of film on the electrode was a problem in some analyses, but this difficulty was easily corrected either by poisoning the electrode or by polishing the electrode surface with a Kimwipe. Probably no truly inert solid electrode exists since the surface is not renewable, unlike, the dropping mercury electrode. During the period of electrolysis changes in the electrode itself are reflected in the current-voltage curve of the electroactive system in solution. Accumulation of electrode products at the stationary electrode produces "extra" electrochemical information.

### 3. REFERENCE ELECTRODE

The reference electrode was of a salt bridge design to minimize the intercontamination of the reference electrode and electrolyte solutions. It is particularly necessary to prevent diffusion entry of the silver ion into the solution because the resulting anodic depolarization could obscure the current voltage curves. The outer glass tube which protected the inner reference electrode from direct contact of the test solution consisted of a 14/23 female ground glass joint at the top and a fine porosity glass frit at the bottom. The inner glass tube had a 14/23 male ground glass joint at the top and was tapered with the end being fitted with an 8-mm porous Vycor plug attached with shrinkable Teflon tubing. To equalize the pressure between the two tubes, a small hole was placed in the outer tube. A silver wire was placed inside the inner tube extending out the top and through a rubber septum cap for ease of connection to the potentiostat clip.



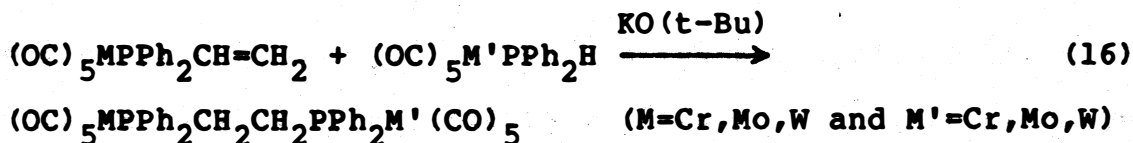
A solution of 0.1 M  $\text{AgNO}_3$  and 0.1 M tetraethylammonium perchlorate (TEAP) in  $\text{CH}_3\text{CN}$  was added to the inner tube by means of a Pasteur pipet. The reference electrode was frequently rinsed and refilled with this solution.

#### 4. AUXILIARY ELECTRODE

The auxiliary electrode consisted of a coiled platinum wire sealed in soft glass tubing 7 mm in diameter. The inside contact to the platinum wire was made by partially filling the tube with mercury and making contact with a copper wire which extended outside the glass tube and was positioned on the upper exterior end of the glass tube. This provided a sturdy and convenient contact for the attachment of the clip lead from the potentiostat.

#### D. REAGENTS and SOLUTIONS

Keiter, Kaiser, and Hansen prepared the homobimetallic and heterobimetallic carbonyl complexes of Cr, Mo, and W which have  $\text{Ph}_2\text{PCH}_2\text{CH}_2\text{PPh}_2$  as a bridging ligand. A base-catalyzed reaction using potassium tert-butoxide was carried out in dry tetrahydrofuran (THF) EQUATION 16. [20]



Two other group VI metal carbonyl complexes were electrochemically studied. The formulas are as follows:



complexes were prepared by Keiter and Mittelberg from the reaction of  $W(CO)_6$ ,  $PPh_3H$  and  $NaBH_4$  in refluxing butanol.

[21]

All reagents were of analytical reagent grade unless otherwise noted. The solvents used were stored in a nitrogen atmosphere glove box to reduce any contamination by oxygen or water. All studies were carried out in methylene chloride solution unless otherwise stated. The stock solutions were prepared by determinate weighing. The solutions were made up in a dry box and transferred to the electrochemical cell either by syringe or directly from the volumetric flask.

## 1. MERCURY

The mercury used for polarography was received already triple-distilled by Bethlehem Apparatus Company and pinholed twice before use.

## 2. SUPPORTING ELECTROLYTE

The supporting electrolyte consisted of 0.1 molar tetrabutylammonium perchlorate (TBAP) in anhydrous methylene chloride. TBAP received from Pfaltz and Bauer Chemicals was recrystallized from ethyl acetate three times and dried in a drying pistol under vacuum over a  $100^{\circ}C$  oil bath. The potential is limited by any presence of water. Therefore, extreme care was taken to make sure the supporting electrolyte was dry. It was stored over Drierite under vacuum until immediately prior to use. The supporting electrolyte was chosen

for the following reasons:

(A) The cathodic range is extended because the quaternary ammonium cation is reduced at a more negative potential than alkali metal cations. [22]

(B) Perchlorate does not depolarize the mercury electrode as do anions such as chloride, which form insoluble salts with mercury. [23]

(C) Since TBAP completely dissociates in methylene chloride, the conductance of the solution is increased. This helps to eliminate any uncompensated  $iR$  drop.

### 3. METHYLENE CHLORIDE

The methylene chloride used was obtained from J. T. Baker or Aldrich Chemical Companies. Prior to use it was refluxed and dried over calcium hydride for at least 24 hours under a nitrogen atmosphere. The dried  $\text{CH}_2\text{Cl}_2$  was then distilled from the  $\text{CaH}_2$  under nitrogen through a 30 cm x 2 cm column packed with glass beads with only the middle seventy percent fraction being used. It was then stored in a nitrogen atmosphere dry box until immediately prior to use. The potential limits to which an electrode can be operated define the utility in terms of the electrochemical systems which can be investigated. The potential limit is reached when the background electrolyte yields current in excess of an arbitrary value (1  $\mu\text{a}$ ). Reactions that operate close to the anodic or cathodic limits are unfavorable. It is unwise to draw too many conclusions about an electrode process which occurs too close to the background cutoff. The ordinary

criteria for nonaqueous solvents include the absence of extraneous background currents and a suitable potential range. The potential range depends on the supporting electrolyte, the electrode material and its surface condition. The tolerance for background currents may depend on the particular measurements carried out. For analytical applications low background and sharp cutoff potentials are needed. If the electroactive species is at high concentration, then the background current is a negligible fraction of the net observable current. In essence this can be described in terms of signal to noise ratio, where the background current corresponds to a noise level or unwanted portion of the total current.

#### 4. NITROGEN

Each electrolytic solution was deaerated for at least 10 minutes by purging with nitrogen before the current-voltage curves were obtained. The nitrogen introduced for deaeration was supplied by Gano Welding of Charleston, Illinois. The dry nitrogen was saturated with methylene chloride by passing through two saturation towers having fine glass frit bubblers. The saturation towers were placed in the water bath having the same temperature as the electrochemical cell. The saturated nitrogen was passed to the electrochemical cell via Pyrex gas lines which were coiled to allow for any flex. Two Teflon spindle stopcocks were used to control the nitrogen gas for deaeration which is bubbled through the

solution before the run and over the solution during the recording of a polarogram or voltammogram.

#### E. EQUIPMENT

The potentiostat employed in these experiments was a Princeton Applied Research Model 173 ( $\pm 100$  V at 1 Amp.). A conventional ramp input was used to provide a linear polarographic sweep, and a Princeton Applied Research Model 175 function generator provided singular triangular wave forms for cyclic voltammetry. Voltammograms were recorded on either a Varian Model F-80 X-Y recorder (used for scan rates below 20 V/min.) or a Tetronix Model 5103N oscilloscope system with Model C-5 camera attachment. The magnitudes of the anodic and cathodic peak current were determined by direct examination of the chart paper or photograph using a 1 mm grid. The cell was equipped with a jacketed water bath for controlling the solution temperature to 20.00°C. The circulating water bath was a Forma Scientific Model 2095. The dry box used was a Vacuum Atmosphere Dri-Lab Glove Box Model HE 43/243 with Dri-train Model HE-493.

#### F. TYPICAL PROCEDURE for CURRENT-CURVES

A 25.00-mL volumetric flask was oven dried at 120°C for at least 24 hours. A solution of millimolar concentration of metal carbonyl and 0.1 molar TBAP in  $\text{CH}_2\text{Cl}_2$  was prepared in the glove box. The solution was transferred from the glove box to the 100-mL electrochemical cell by a 50-mL syringe with a 10-cm needle. Prior to the transfer of the solution,

the empty cell was purged with nitrogen for at least 20 minutes, the electrochemical cell being maintained at 20.00°C. After addition, the solution was deaerated for at least 10 minutes with nitrogen. The cyclic voltammograms were obtained at a variety of scan rates with the entire potential range being observed. Beginning at zero volts, the scan went cathodically until discharge was reached and then the scan was reversed in the positive (anodic) direction until discharge and finally was brought back to the initial potential of zero volts. The solution was stirred by the glass frit bubbler after each voltammogram.

### III. RESULTS and DISCUSSION

Properties to be investigated are the controlling process for the limiting current, the number of electrons involved in the oxidation or reduction and the reversibility of the oxidation or reduction.

#### 1. FERROCENE as an INTERNAL STANDARD

##### A. CYCLIC VOLTAMMETRY of FERROCENE

Polarography and cyclic voltammetry, the two methods employed in this study, are excellent techniques for the characterization of new compounds. The basic thermodynamic quantity assigned to an electrode process is the standard electrode potential,  $E^0$ , which is usually written as a reduction and can be found in most reference tables. [24] In aqueous solution the measurement of reduction potentials is made by using reliable and universally accepted reference electrodes such as the normal hydrogen electrode (NHE) or the saturated calomel electrode (SCE). [25] In the present study the electrochemical measurements could not be made in aqueous solution because of the insolubility of the carbonyl compounds. Unfortunately, there is no universal reference electrode that exists for nonaqueous solvents such as methylene chloride. [26] A practical approach to this problem is the use of the potential of the oxidation of ferrocene as an internal standard. The peak currents and position of the waves of the group VI metal carbonyls can be directly compared to the potential of the ferrocenium/ferrocene

(Fe<sup>+</sup>/Fe) couple. FIGURE 1 illustrates a cyclic voltammogram of ferrocene in methylene chloride with 0.1 molar tetrabutylammonium perchlorate (TBAP) vs. Ag/AgNO<sub>3</sub> reference electrode. A formal potential of +0.15 volts was found for this system and was calculated using EQUATION 17.

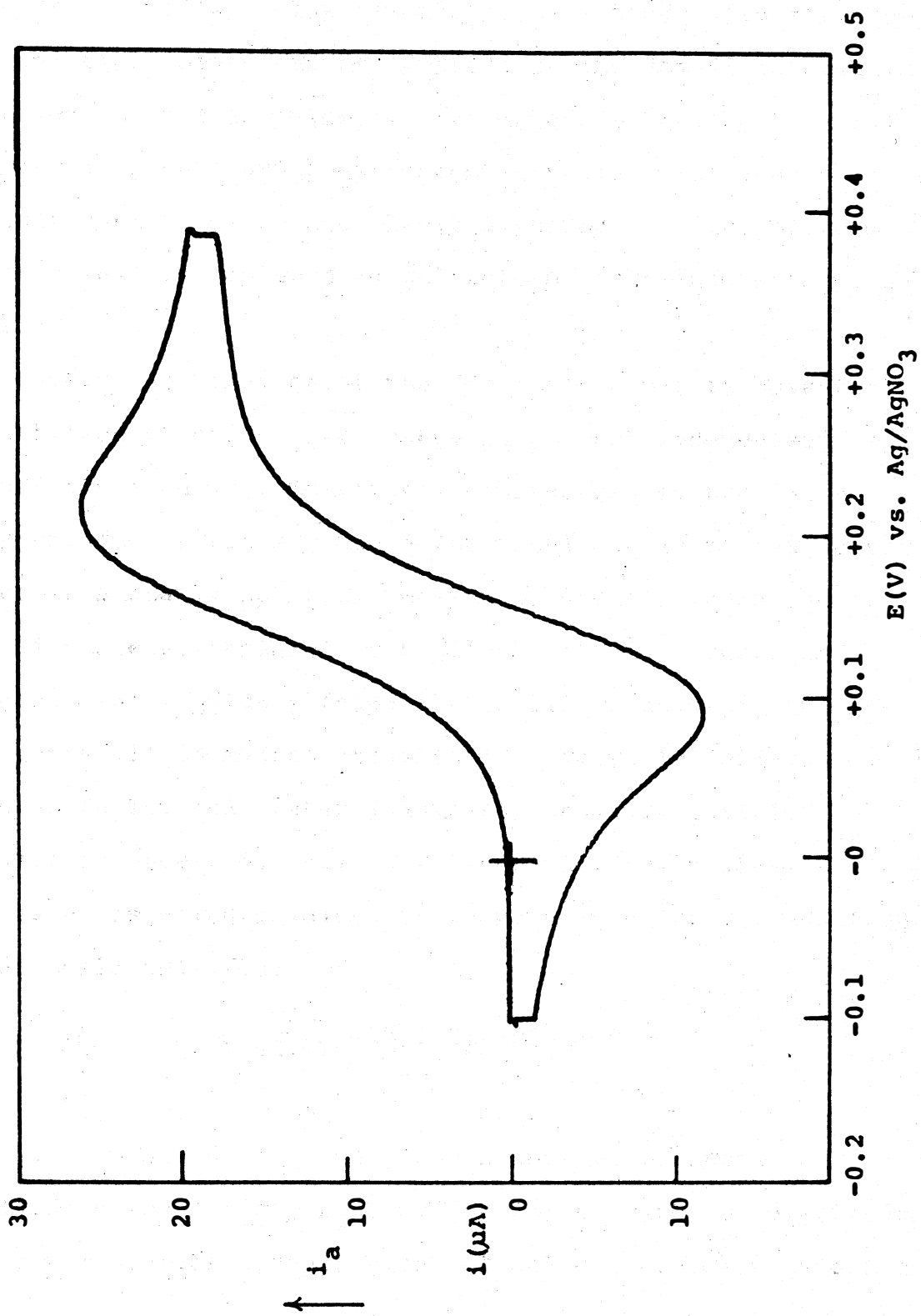
$$E^{\circ} = (E_{p(\text{anodic})} + E_{p(\text{cathodic})}) / 2 \quad (17)$$

In similar systems used by Hershberger and Bond, E<sup>o</sup> values for ferrocene of +0.31 volts versus saturated NaCl SCE and +0.50 volts versus Ag/AgCl were determined. [27,28] The discrepancies can be attributed to the different reference electrodes used. An important advantage of this method is that the choice of the reference electrode used to satisfy the three-electrode potentiostat is reduced to a matter of experimental convenience. The use of different reference electrodes will shift the waves along the potential axis, but the formal potentials relative to E<sup>o</sup>(Fe<sup>+</sup>/Fe) couple will remain unchanged. The formal potentials should be reproducible because the variables such as liquid junction potentials and reference electrode degradation are eliminated.

The (Fe<sup>+</sup>/Fe) couple (E<sup>o</sup> = 0.400 V vs. NHE) may not be a satisfactory internal standard if the anodic or cathodic limits are reached before the oxidation or reduction of ferrocene. [29] In this case other compounds such as cobaltocene (E<sup>o</sup> = -0.918 V vs. NHE) can be substituted. [30]



FIGURE 1. Voltammogram of  $6.0 \times 10^{-4}$  M ferrocene  
in a 0.10 M TBAP-methylene chloride solution  
(1.0 V/min.).



The oxidation-reduction of ferrocene ideally falls in between the anodic and cathodic limits of this methylene chloride (with TBAP) system.

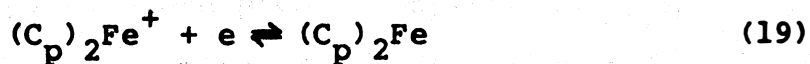
The use of ferrocene as an internal standard in electrochemical experiments can be compared to the use of internal standards in nuclear magnetic resonance spectroscopy. For example, in proton NMR spectroscopy tetramethylsilane is commonly used to reference chemical shifts of other protons but is sometimes replaced by chloroform to avoid overlapping signals.

Reversible behavior of the ( $\text{Fe}^+/\text{Fe}$ ) couple is observed in methylene chloride. Ferrocene is solvent independent because the iron is symmetrically surrounded by the large cyclopentadienyl rings. Since the metal ion is buried at the center of a nearly spherical molecule, the oxidation and reduction are accompanied by negligible chemical and steric changes. [31] Delahay found that cyclic voltammetry at slow scan rates (10-50 mV/sec) results in reversible behavior, while at faster scan rates ( $>1$  V/sec) quasi-reversible behavior is observed. [32] For linear diffusion where ferrocene was being oxidized or reduced in solution, EQUATION 18 was followed. [33]

$$i_p = 2.72 \times 10^5 n^{3/2} A D^{1/2} C v^{1/2} \quad (18)$$

where  $i_p$  = peak current ( $\mu\text{A}$ );  $n$  = number of electrons involved in the oxidation or reduction;  $A$  = area of electrode ( $\text{cm}^2$ );  $D$  = diffusion coefficient of the electroactive species

( $\text{cm}^2\text{sec}^{-1}$ );  $C$  = concentration of the electroactive species in solution (mmoles/L);  $V$  = sweep rate ( $\text{Vsec}^{-1}$ ). A typical single sweep cyclic voltammogram, (See FIGURE 1), used in this study was of one forward sweep and one reverse sweep with the switching potential not less than about 35 mV. Bard found that for switching potentials close to the anodic peak, the shape of the cathodic wave may be affected. [34] For a reversible system such as ferrocene, where the fast electron transfer was accompanied by slow chemical reactions, the ratio of the heights of the cathodic peak,  $i_{p_c}$ , and the anodic peak,  $i_{p_a}$ , is unity. Also for a reversible system, the separation of the peak potentials,  $\Delta E_p$ , was 59 mV. If the electron transfer reaction was irreversible, then the peak to peak distance was increased. A third criterion for reversibility requires the peak potential,  $E_p$ , to be independent of scan rate, and  $i_p$  to be proportional to  $V^{-1/2}$ . The latter property indicates diffusion control and is analogous to the variation of  $i_d$  with  $(h)^{1/2}$  in polarography. A list of the above values can be found in TABLE 1. The magnitude of the peak currents can be used to compare the number of electrons transferred in the metal carbonyl systems because ferrocene is a known one-electron transfer (EQUATION 19).



From the values listed in TABLE 1 ferrocene exhibits reversible behavior. The ratio of the anodic and cathodic peak currents are unity and the anodic peak potentials are independent of scan rate.

TABLE 1. VOLTAMMETRIC DATA of FERROCENE

SCAN RATE (V/min.)	$E_{pa}$ (V)	$E_{pc}$ (V)	$E^0$ (V)	$\Delta E_p$ (mV)	$i_{pa}$ ( $\mu A$ )	$i_{pc}$ ( $\mu A$ )	$i_{pa}/i_{pc}$ ---
1.0	0.190	0.105	0.148	85	15.89	17.12	0.93
2.0	0.190	0.098	0.144	92	21.29	23.38	0.91
5.0	0.198	0.088	0.143	110	32.58	28.57	1.14
10.0	0.207	0.077	0.142	130	44.88	42.81	1.04

## B. POLAROGRAPHY OF FERROCENE

In polarography the current can be solely limited by diffusion. In this case the limiting current,  $i_L$ , is proportional to  $m^{2/3}t^{1/6}$ , where (m) is the rate of flow of mercury through the capillary of the dropping mercury electrode expressed in milligrams per second and (t) is the drop time in seconds. The drop time is inversely proportional to the height of the mercury column, ( $h_{corr}$ ), corrected for back pressure due to the interfacial tension at the drop surface, and (m) is directly proportional to ( $h_{corr}$ ). The current is proportional to the area of the electrode, and since the area is directly proportional to  $m^{2/3}t^{1/6}$ , the limiting current,  $i_L$ , was then proportional to ( $h_{corr}$ )<sup>1/2</sup>. From these considerations a plot of  $\log(i_L)$  versus  $\log(h_{corr})$  will indicate the limiting current is diffusion controlled if the slope is 0.50. Once diffusion has been established as the limiting process, then the diffusion current,  $i_d$ , may be related to the number of electrons involved in the

process (n), the diffusion coefficient (D), concentration of the electroactive species (C), mass flow rate (m) and time (t) by the Ilkovic equation (Equation 20). [35]

$$i_d = 706nCD^{1/2}m^{2/3}t^{1/6} \quad (20)$$

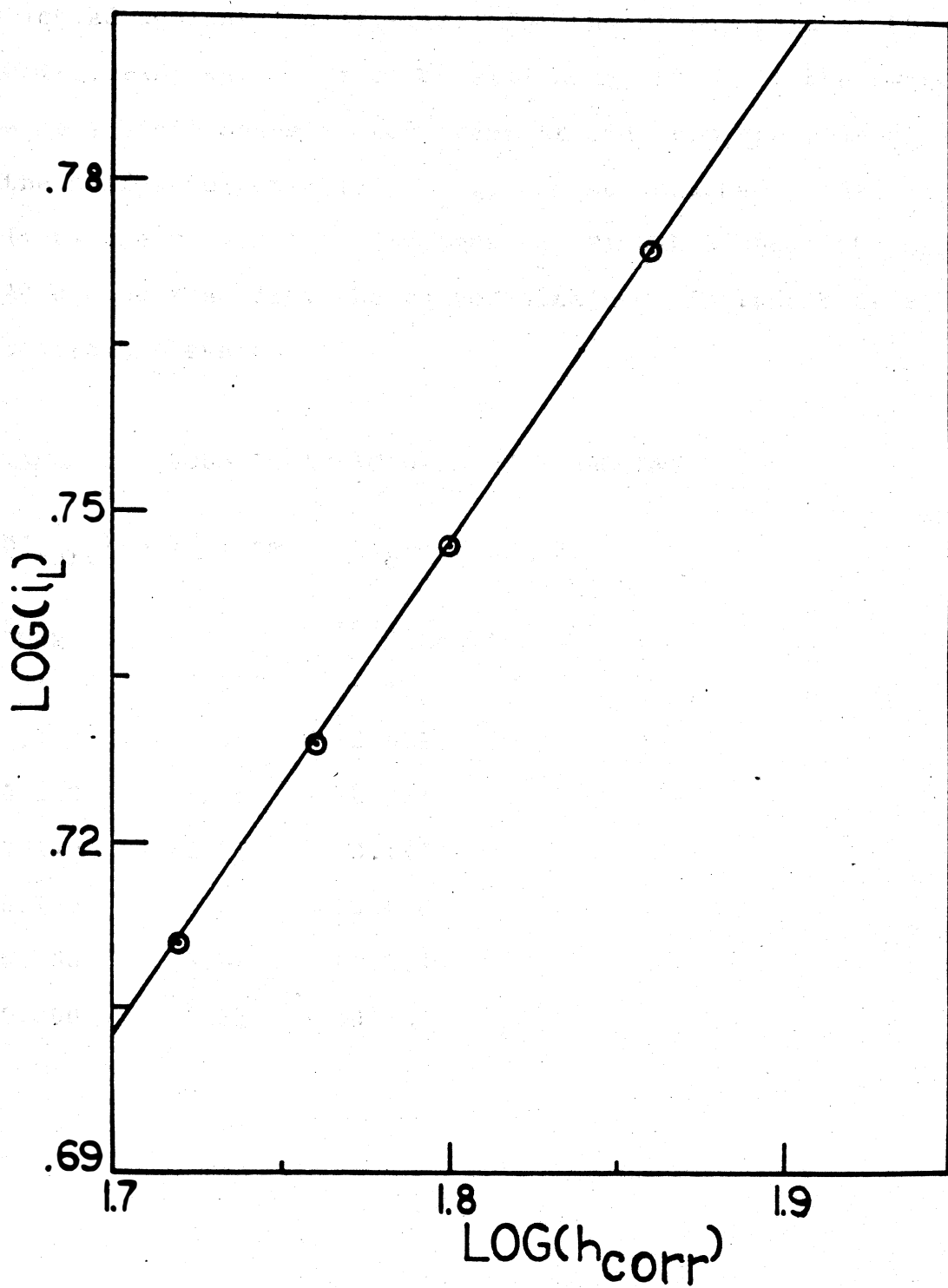
The capillary characteristics for the dropping mercury electrode were:  $m = 1.660$  mg/sec and  $t = 122$  sec. The diffusion coefficient of the oxidation of ferrocene was  $2.3 \times 10^{-5}$  cm<sup>2</sup>/sec which is in agreement with that found by Kuwana. [13] Polarographic data are given in TABLE 2 for ferrocene and a plot of  $\log(i_L)$  versus  $\log(h_{corr})$  is given in FIGURE 2. A slope of 0.48 obtained from this investigation indicated that diffusion is the rate controlling process for the oxidation of ferrocene.

TABLE 2. POLAROGRAPHIC DATA of FERROCENE

$E_{1/2}$ (V)	$i_L$ ( $\mu$ A)	LOG( $i_L$ ) -----	$h$ (cm)	$h_{(corr)}$ (cm)	LOG[ $h_{(corr)}$ ] ----
0.14	5.98	0.777	74.9	73.2	1.86
0.14	5.58	0.747	64.7	63.1	1.80
0.15	5.35	0.728	59.6	58.0	1.76
0.14	5.12	0.709	54.0	52.4	1.72

A further check for reversibility has been provided by Meites who showed that the assumption of thermodynamic reversibility for an electrode process leads to the following relationship. [36]

**FIGURE 2. Diffusion control plot of ferrocene.**





$$E_{DME} = E_{1/2} + 0.059/n \log[(i_d - i)/i] \quad (21)$$

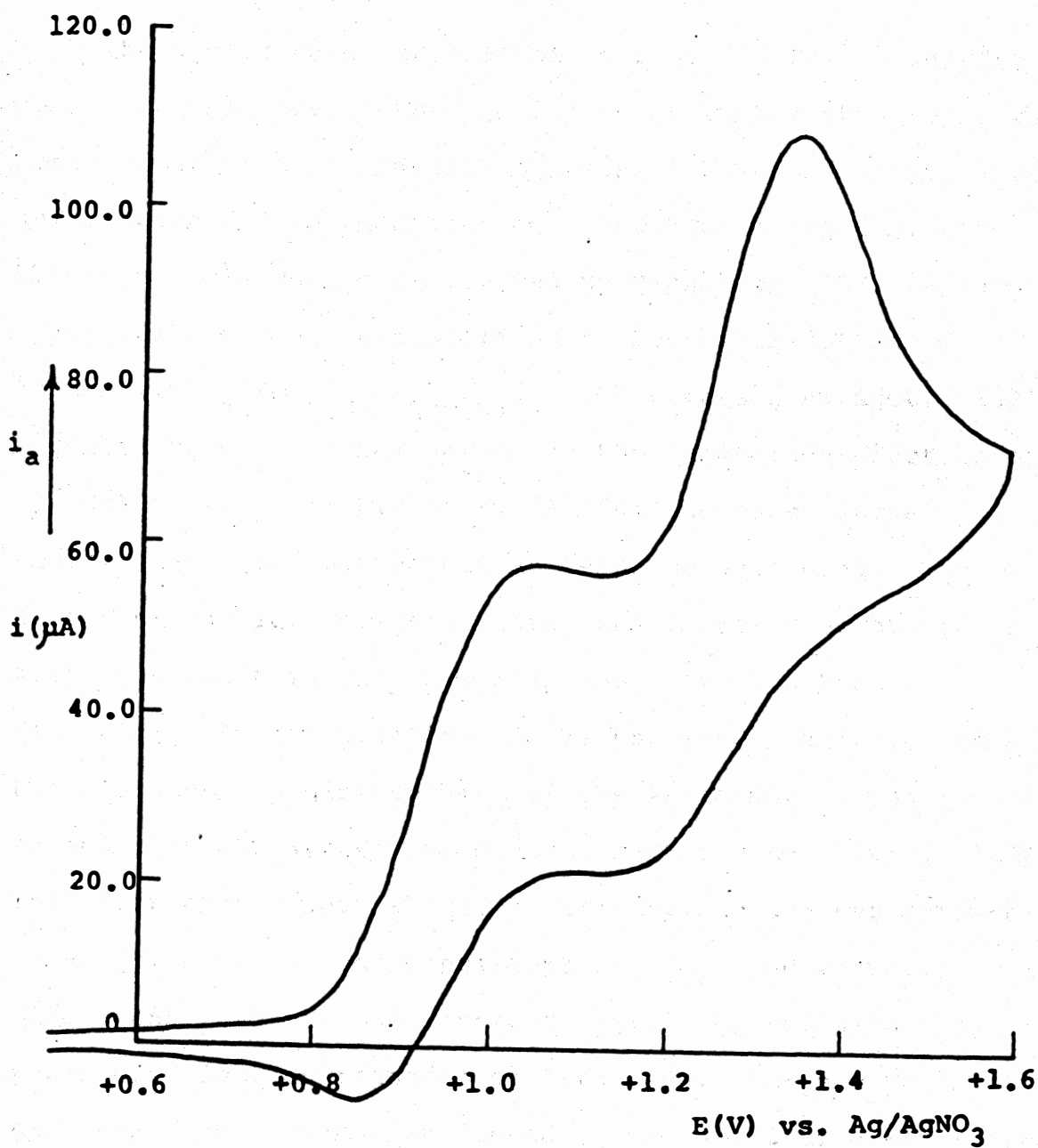
If  $E_{DME}$ , the potential of the dropping mercury electrode is plotted against  $\log[(i_d - i)/i]$  for the rising part of the polarograph wave, the slope will equal 59 mV if the system is a reversible one-electron transfer and from the y-intercept the half-wave potential,  $E_{1/2}$ , can be obtained. TABLE 3 lists the values for ferrocene and FIGURE 3 shows the plot. As can be seen from the values obtained, ferrocene is a reversible system.

TABLE 3. POLAROGRAPHIC DATA of FERROCENE

$$h(\text{corr}) = 77.1 \text{ cm} \quad i_d = 6.13 \mu\text{A}$$

$E_{DME}$	$i$	$\text{LOG}(i/i_d - i)$
(V)	( $\mu\text{A}$ )	-----
0.120	1.45	-0.509
0.130	1.95	-0.331
0.140	2.55	-0.147
0.150	3.20	+0.038
0.160	3.84	+0.224
0.200	5.35	+0.836

FIGURE 3. Plot of EQUATION 5. Reversibility,  $n$  and  $E_{1/2}$  determination of ferrocene.



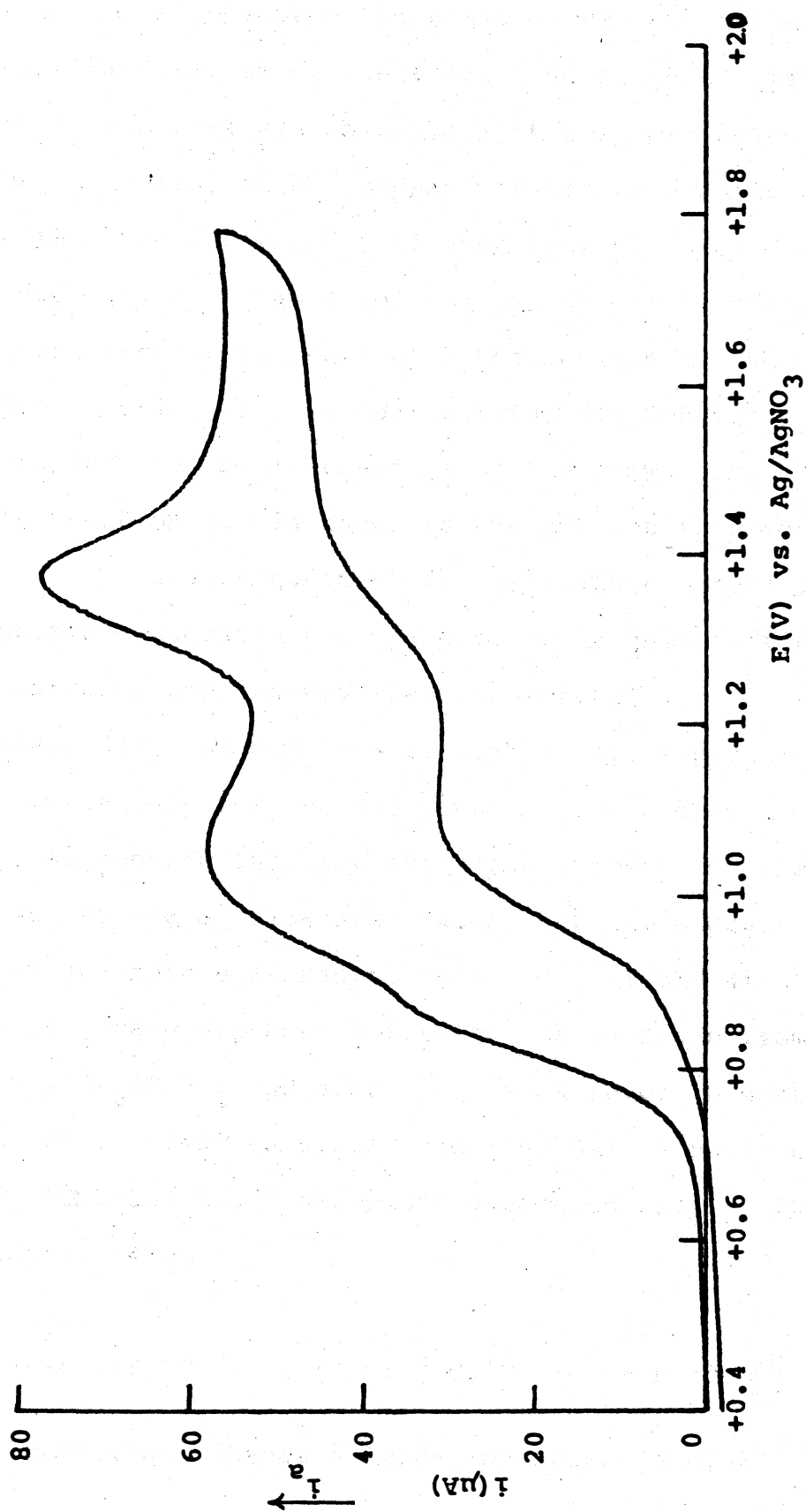
## 2. CYCLIC VOLTAMMETRY of GROUP VI METAL CARBONYLS

### A. HOMOMETALLIC COMPLEXES

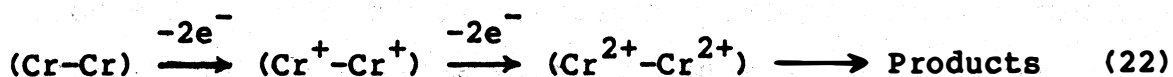
#### 1. $(OC)_5CrPPh_2CH_2CH_2PPh_2Cr(CO)_5 = (Cr-Cr)$

The cyclic voltammetric behavior of (Cr-Cr) in anhydrous methylene chloride containing 0.1 molar (TBAP) at 20.00°C was observed in order to obtain both qualitative and quantitative information on its oxidation and reduction mechanism. The theory of this method is treated by Nicholson. [37] A report by Bagchi revealed reversible one-electron oxidation of  $trans-Cr(CO)_4(PPh_3)_2$  with  $E_{pa} = 0.72$  V versus Ag/AgCL. [38] A typical cyclic voltammogram for the oxidation-reduction of (Cr-Cr) is shown in FIGURE 4. A sigmoid-shaped curve exhibiting a somewhat Nernstian response was found. The linear triangular potential sweep was initialized at zero volts and swept in the increasing negative (cathodic) direction. At the negative limit, the sweep was reversed and the positive (anodic) portion of the voltammogram was recorded and then the system was brought back to the initial limit. The first anodic peak showed a well-defined current maximum at +1.07 volts and was consistent with two one-electron oxidations when the peak currents were compared with the known one-electron transfer of ferrocene. The second anodic peak had a current maximum found at +1.35 volts, again corresponding to two one-electron transfers. On reversal, one cannot discern the cathodic peak for the second anodic wave, at least for slow sweep rates (1.0 V/min.). At faster sweep rates (>5.0 V/min.), the cathodic peak for the second

FIGURE 4. Voltammogram of  $5.47 \times 10^{-4}$  M  
 $(OC)_5CrPPh_2CH_2CH_2Ph_2PCr(CO)_5$   
in a 0.10 M TBAP-methylene  
chloride solution.  
(5.0 V/min.)



anodic wave becomes more apparent and the peak current corresponds to two one-electron transfers. The cathodic peak coupled to the first anodic wave was also two one-electron transfers. This peak was observable at all scan rates. The fact that the second cathodic peak was not observable unless the scan rate was increased indicates that the second oxidation product was not stable for the period of the measurement at slow scan rates. Inspection of the details of the sweep dependence reveals that the peak current for the first and second anodic wave was independent of the sweep rate (TABLE 4). This relationship is known as the current function,  $i_p/v^{1/2}$ , and should be constant for reversible behavior. The values obtained suggest that the electron transfer from this (Cr-Cr) carbonyl complex was electrochemically quasi-reversible. [39] Examination of look at the separation of the peak potentials for the first wave shows a decrease in the,  $\Delta E_p$ , suggesting that the oxidation product for the first wave is not stable at slow scan rates, but the process becomes more reversible at faster scan rates (TABLE 4). Bond reported scan rate dependence for the cis to trans isomerization of  $\text{Cr}(\text{CO})_2(\text{DPM})_2$  and also reported a reversible second oxidation step. [40] A system such as this is best described by EQUATION 22. Nicholson described this as Case VI in his paper. [41]



The electrochemical standard oxidation potentials,  $E^0$ , varied

from 0.96 V to 0.94 V for the first wave (TABLE 4). Cyclic voltammetric data were collected over the range of scan rates of 1.0 to 20.0 V/min. The current voltage measurements of the peak separations confirm the electrochemical quasi-reversible behavior of the (Cr-Cr) redox couple (TABLE 4). Also, the fact that the ratio of the anodic peak current to the cathodic peak current did not equal unity was another indication of the deviation from reversibility (TABLE 4).

TABLE 4. VOLTAMMETRIC DATA of  $(OC)_5CrPPh_2CH_2CH_2Ph_2PCr(CO)_5$

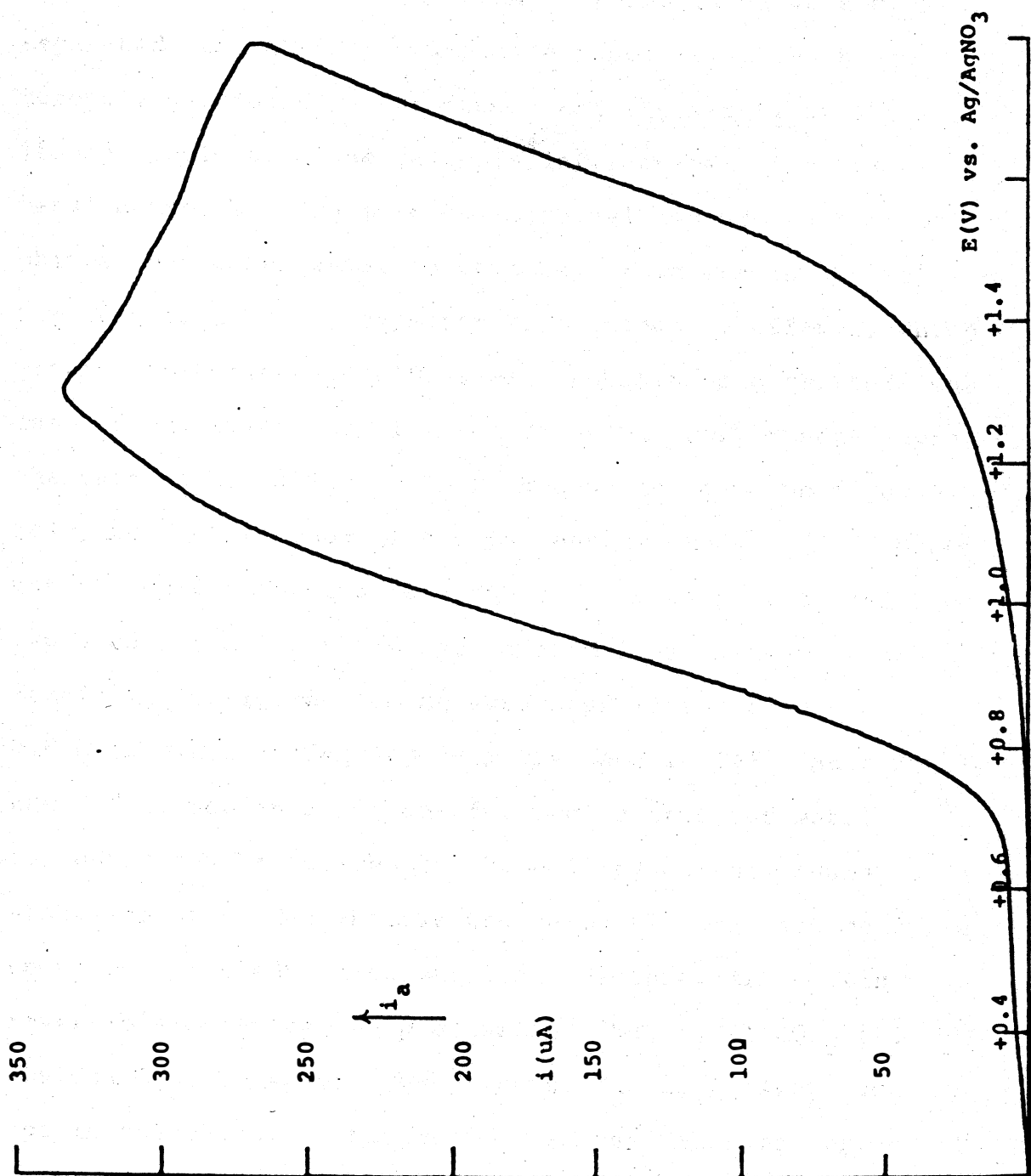
SCAN RATE (V/min.)	$E_{pa}$ (V)	$E^0$ (V)	$i_{pa}$ ( $\mu A$ )	$i_{pc}$ ( $\mu A$ )	$i_{pa}/i_{pc}$ ----
1.0	1.07	0.96	41.61	30.71	1.35
2.0	1.05	1.03	48.03	-----	-----
5.0	1.03	0.94	54.92	44.88	1.22
10.0	1.03	0.94	74.80	58.27	1.28
20.0	1.04	0.94	117.9	72.83	1.62

#### A. ADDITION of EXCESS LIGAND $Ph_3P$

The cyclic voltammogram of the (Cr-Cr) complex at fast sweep rates ( $> 5.0$  v/min) consists of two quasi-reversible waves. However, when 2.1 moles of  $Ph_3P$  was added to a solution containing  $4.8 \times 10^{-4}$  molar (Cr-Cr), the cathodic waves were absent and was replaced by two new irreversible waves (FIGURE 5). This indicates possible substitution of the oxidized (Cr-Cr) species by  $Ph_3P$ . When larger amounts of  $Ph_3P$  were employed, both anodic waves merged into one drawn-

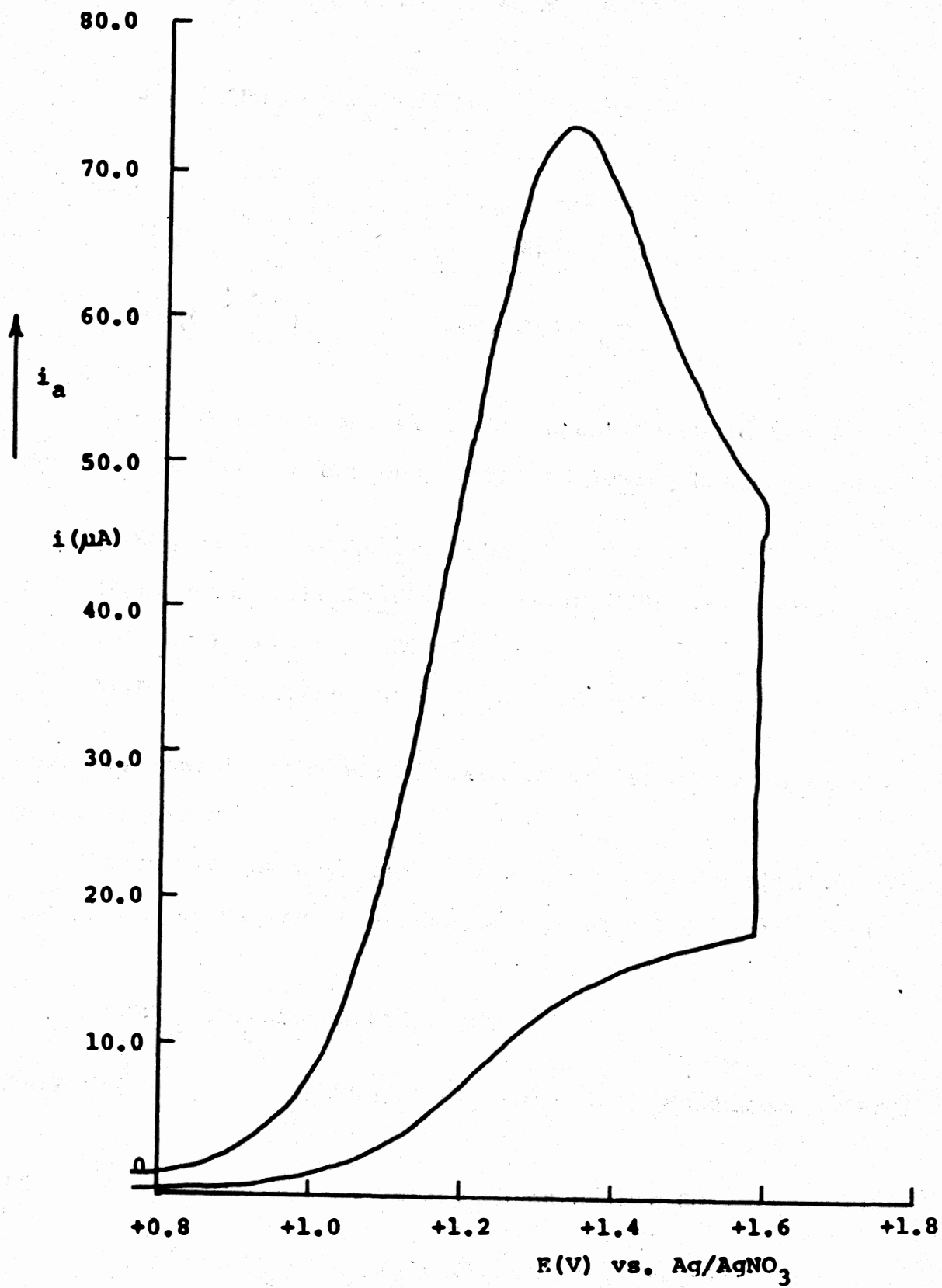


FIGURE 5. Voltammogram of  $4.80 \times 10^{-4}$  M  
 $(OC)_5CrPPh_2CH_2CH_2Ph_2PCr(CO)_5$   
and  $1.00 \times 10^{-3}$  M  $Ph_3P$  in a  
0.10 M TBAP-methylene chloride  
solution.

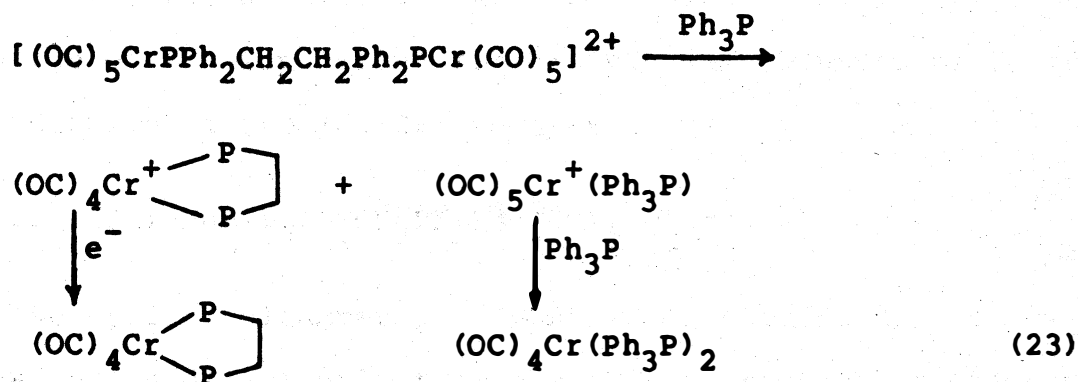


out wave (FIGURE 6). The substitution by  $\text{Ph}_3\text{P}$  of the (Cr-Cr) complexes is more difficult to interpret solely on the basis of the cyclic voltammograms since the anodic and cathodic waves are not cleanly separated. If the waves were cleanly separated, the standard oxidation potentials, which are strongly dependent on the number and the nature of the ligand, could disclose valuable information. The (Cr-Cr) metal center bearing more non-carbonyl ligands such as phosphines should be easier to oxidize. This was in accord with the results normally expected from inductive effects, which predict that electron withdrawing substituents decrease the ease of oxidation and electron donating substituents increase the ease of oxidation.  $\text{Ph}_3\text{P}$  is considered to be a good  $\pi$ -acid, but not as good as the carbonyl ligands. [42] Substitution usually stops after two or three carbonyls have been replaced for all but the best  $\pi$ -acid ligands because the remaining CO ligands become saturated in their ability to withdraw electron density from the metal. [43] Accordingly, the difference in  $E^\circ$  values for the substituted metal carbonyls can be related to the ability of the ligands to stabilize or to destabilize the carbonyl metal cation formed upon two one-electron oxidations. Hershberger reports a reversible one-electron process for  $(\text{MeCN})(\text{Cr})(\text{CO})_5$  and  $(\text{Py})\text{Cr}(\text{CO})_5$ . However, when excess  $\text{Ph}_3\text{P}$  is present each cyclic voltammogram changes to what can be characterized as irreversible. He suggests the electrode process consists of a reversible charge transfer followed by chemical regeneration of the reduced complex. [44]

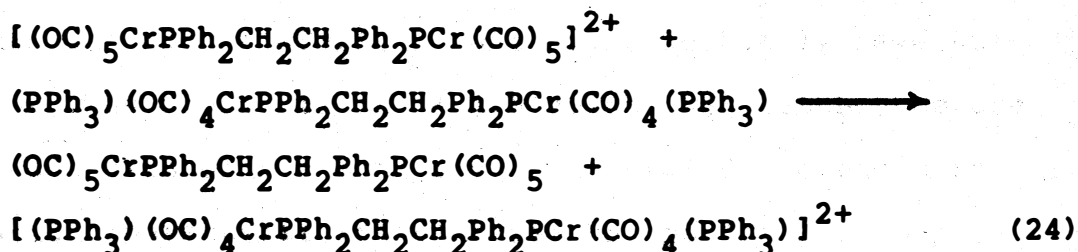
FIGURE 6. Voltammogram of  $5.62 \times 10^{-4}$  M  
 $(OC)_5CrPPh_2CH_2CH_2Ph_2PCr(CO)_5$   
and  $9.94 \times 10^{-2}$  M  $Ph_3P$  in a  
0.10 M TBAP-methylene chloride  
solution.



One possible reaction could be EQUATION 23.

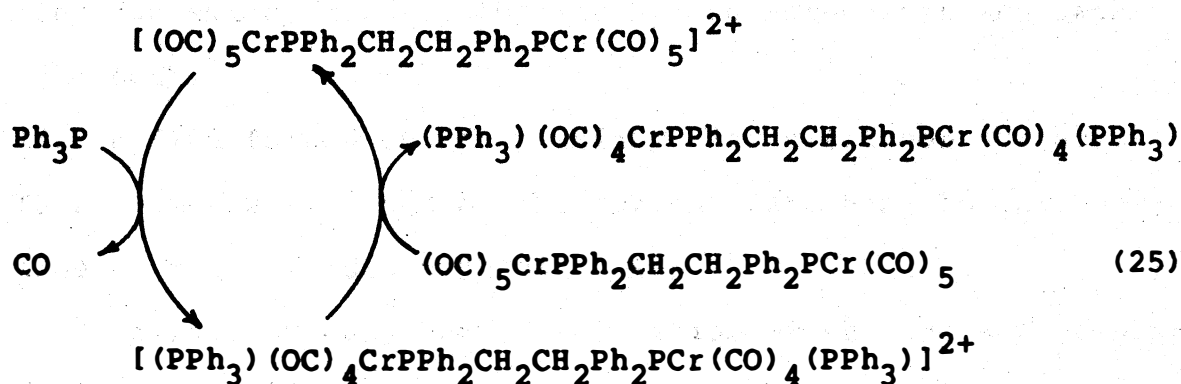


The  $E^0$  values which were more positive could thermodynamically favor reactions of the following kinds to occur.

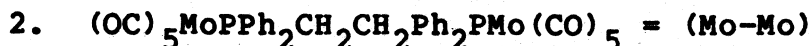


However, whether they will indeed occur depends upon kinetic considerations.

There was not any sign of a catalytic cycle although similar systems have been documented (EQUATION 25). [45]



The (Cr-Cr) species could not be reduced at voltages down to -2.2 volts using the dropping mercury electrode. Discharge of the supporting electrolyte was observed prior to any reduction of the (Cr-Cr) complex.



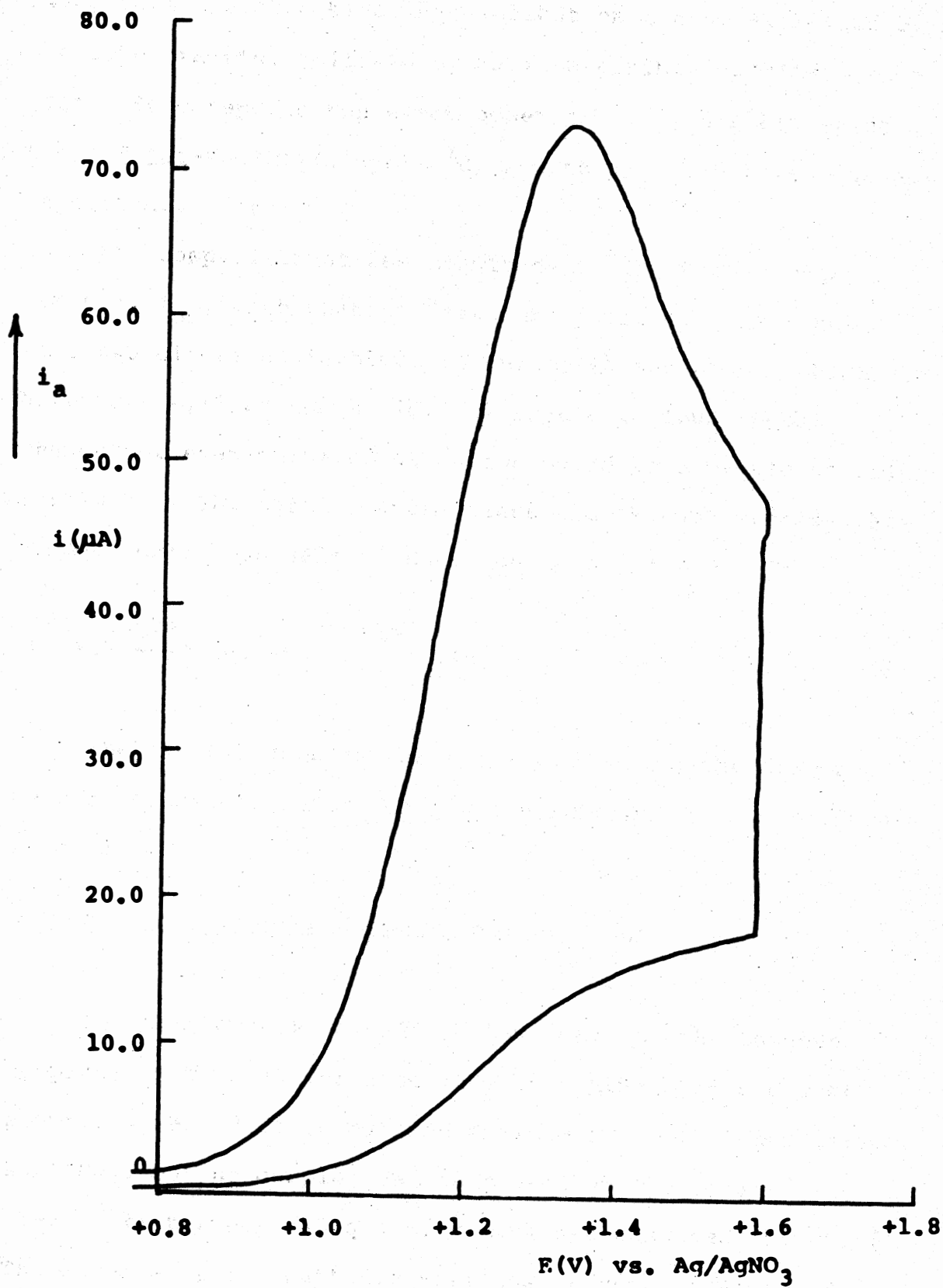
The cyclic voltammetry (FIGURE 7) of the (Mo-Mo) complex behaved quite differently from the (Cr-Cr) species in that it showed a single oxidation wave at +1.06 volts versus Ag/AgNO<sub>3</sub> along with no coupled cathodic peak. The appearance of the shape of the single peak indicates that the electron transfer process was not as simple as one might initially have suspected. The anodic limit (+ 1.8 volts) was reached before any indication of a second wave. Several differences in the oxidation characteristics compared to the (Cr-Cr) complex were noted:

- (1) The oxidation peak potential,  $E_{\text{pa}}$ , shifted in the positive direction by +0.2 volts versus Ag/AgNO<sub>3</sub>.
- (2) One anodic wave was observed instead of two.
- (3) The (Mo-Mo) redox couple showed a considerable degree of electrochemical irreversibility by the absence of the cathodic peak.
- (4) A film formed on the platinum disc electrode surface. This film was detected by the current returning to the baseline on the reversed cathodic sweep.

It was obvious that the oxidation of the (Mo-Mo) complex was accompanied by some kinetic complications and the oxidized species was not stable for the time period of the

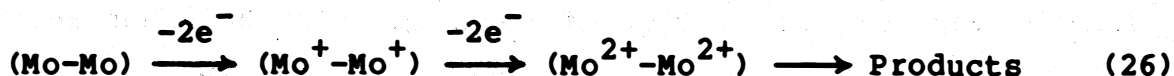
**FIGURE 7. Voltammogram of  $4.73 \times 10^{-4}$  M**  
 **$(OC)_5MoPPh_2CH_2CH_2Ph_2PMo(CO)_5$**   
**in a 0.10 M TBAP-methylene**  
**chloride solution.**  
**(5.0 V/min.)**



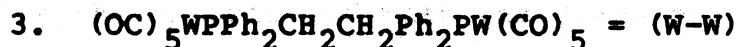


sweep rate. Such a kinetic complication can be explained by a charge transfer followed by an irreversible chemical reaction. Bond reports the electrochemical irreversible oxidation of  $\text{mer-Mo(CO)}_3(\text{n}^1\text{dpm})(\text{n}^2\text{dpm})$  with  $E_{\text{pa}} = 0.24 \text{ V vs. Ag/AgCl}$  in acetone. [46]

The comparison of the magnitude of the anodic peak current,  $i_{\text{pa}}$ , with that of ferrocene indicates that there were two electrons involved in the oxidation step, which was a feature similar to the (Cr-Cr) species. Thus "equal chance" or even numbered oxidation would be expected to occur for both of the metal centers since the (Mo-Mo) species were symmetrically equivalent (Equation 26). [47]

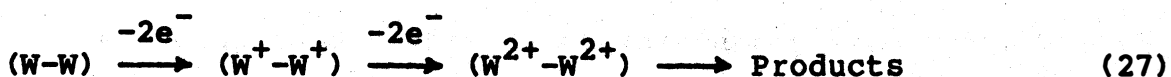


The (Mo-Mo) complex was not reducible on the dropping mercury electrode before cathodic discharge of -2.0 volts was reached.



The single sweep cyclic voltammogram of the tungsten complex, (W-W), was characterized by a single anodic wave showing a well defined current maximum at +1.12 volts versus  $\text{Ag/AgNO}_3$ , but no coupled cathodic wave on the reverse scan even at fast sweep rates (20.0V/min) was observed (FIGURE 8). The absence of the cathodic wave was evidence that the electron transfer from the (W-W) carbonyl was electrochemically

irreversible. This absence of the reverse electron transfer step results from the rapid decomposition of the cation. In a similar system, Hershberger found an irreversible one-electron oxidation for  $(\text{Ph}_3\text{P})\text{W}(\text{CO})_5$ . [48] Comparison of the magnitude of the anodic peak current,  $i_{\text{pa}}$ , with that of ferrocene suggests two one-electron oxidations were occurring just as for the other metals in this series (Equation 27).



The anodic peak potential,  $E_{\text{pa}}$ , for the (W-W) species was 0.06 volts more positive than that for the (Mo-Mo) complex and 0.08 volts more positive than that for the (Cr-Cr) complex. Therefore, in this series of group VI metal carbonyls, the metal center which was easiest to oxidize was the (Cr-Cr) complex, followed by the (Mo-Mo) species and finally the (W-W) complex. Tungsten metal having the largest atomic radius would seem to be the easiest to oxidize, which was exactly the opposite of what was discovered. Pauling's electronegativity for this series of group VI metals is approximately the same for all members. Therefore, no relationship can be made between ease of oxidation and electronegativity. [49] Kochi found for tris(acetonitrile) complexes, the standard oxidation potential for the metal center decreased in the order  $\text{Mo} > \text{W} > \text{Cr}$ . [50] This same order was determined by Bond for a series of dicarbonylbis(diphenylphosphino)-methane complexes. [51] This experiment suggests the ease

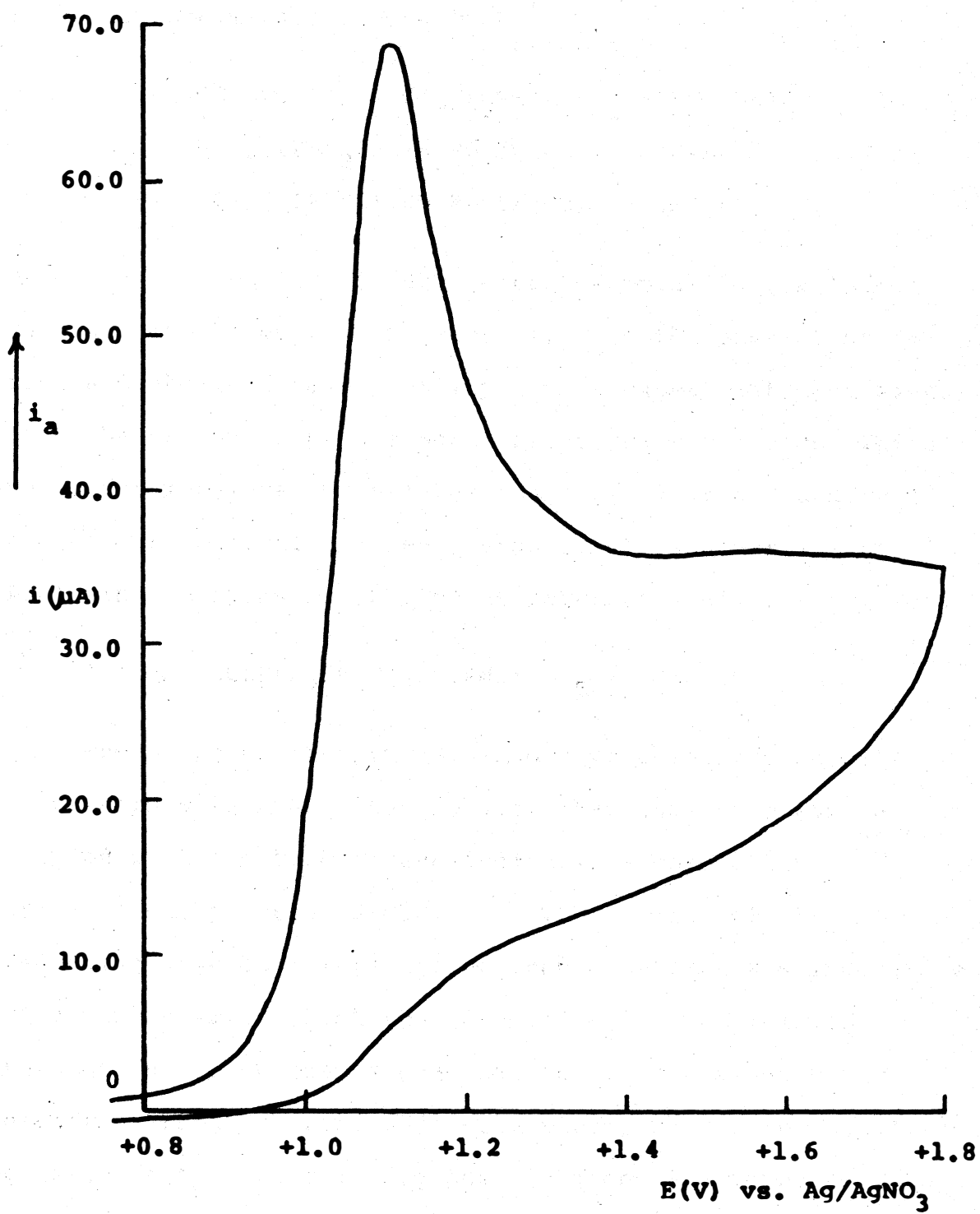
of oxidation depends on both reactant and product stability. The (W-W) and (Mo-Mo) complexes both give unstable products, whereas the (Cr-Cr) product is stable.

Kinetic complications were suggested by the current returning to the baseline on the cathodic sweep. This feature of the cyclic voltammogram was explained by the formation of a film on the electrode surface. This behavior was also found in the (Mo-Mo) complex.

A second anodic peak at approximately +1.7 volts was found which was characteristic of an adsorption peak. This was determined by the symmetry of the wave itself and by the fact that the current did not decay with a  $t^{1/2}$  relationship. [52,53] The term stripping peak is also used to describe the wave arising from the oxidation or reduction of the film formed at the electrode surface. This adsorption peak was a feature in the (W-W) system, but was discovered only with increasing sweep rate. Therefore, the lifetime of the oxidized species must be very short lived before the reaction which leads to the development of the film on the electrode surface occurs. In some cases, such as the oxidation of the (Mo-Mo) complex, the formation of a film occurs on the electrode surface, but the stripping peak for this film was absent. Instead, the current decays to the original baseline on the reverse cathodic sweep. The film remained on the electrode surface and was removed by polishing the electrode surface.

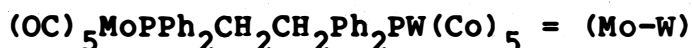
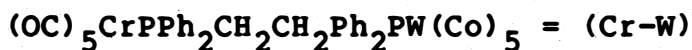
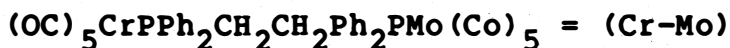
The (W-W) complex was not reducible on the dropping mercury electrode before the cathodic discharge was reached.

FIGURE 8. Voltammogram of  $4.44 \times 10^{-4}$  M  
 $(OC)_5WPh_2CH_2CH_2Ph_2PW(CO)_5$   
in a 0.10 M TBAP-methylene  
chloride solution.  
(5.0 V/min.)

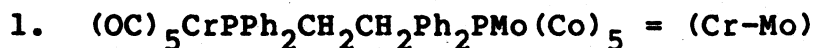


## B. HETEROBIMETALLIC COMPLEXES

The cyclic voltammograms were obtained for the following three heterobimetallic complexes:



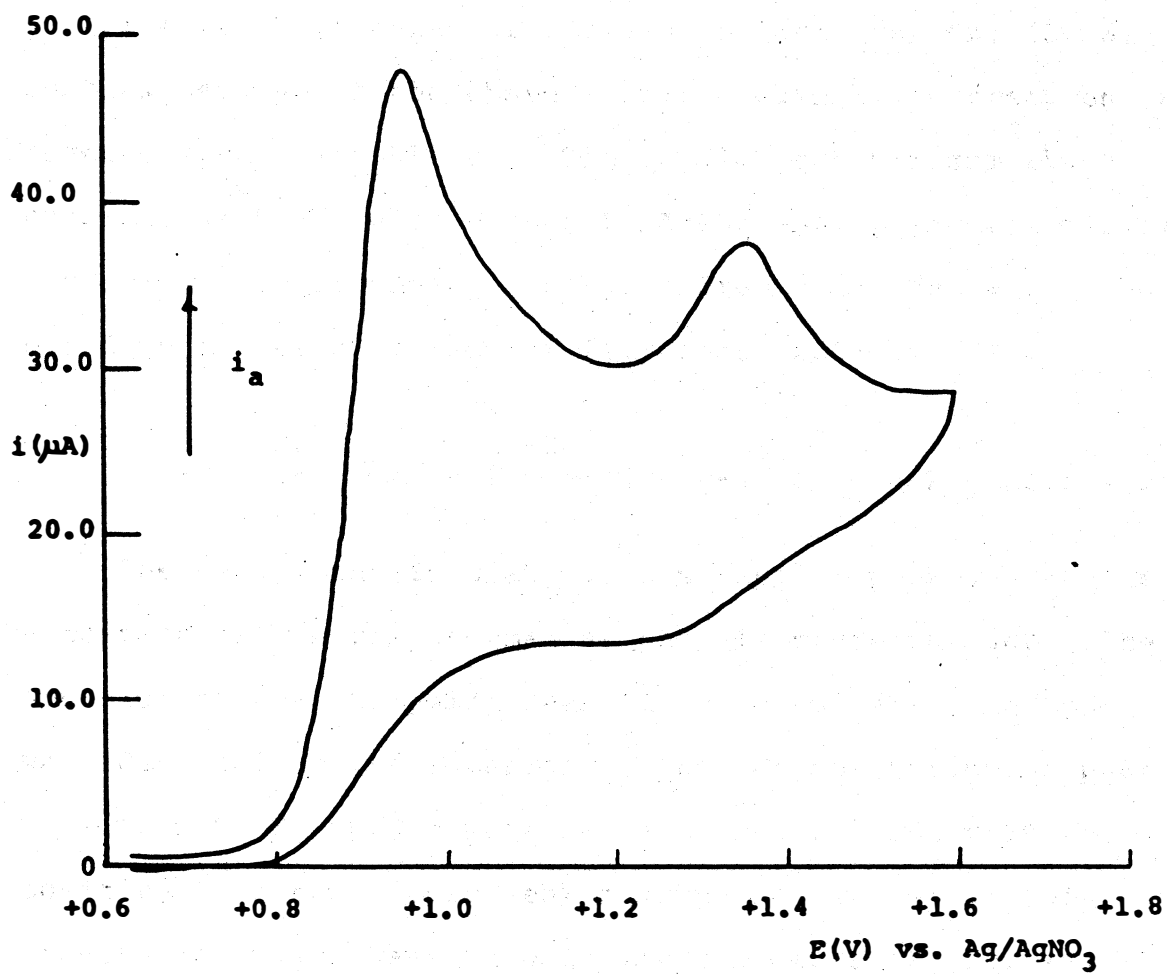
Based on the results for the three homometallic complexes several comparisons can be made, such as the ease of oxidation and chemical reversibility. This experiment determined that the oxidation of one metal center does not occur while the other metal center remains neutral. A brief summary of the electrochemical and redox properties is given in the following sections for the three heterobimetallic complexes.

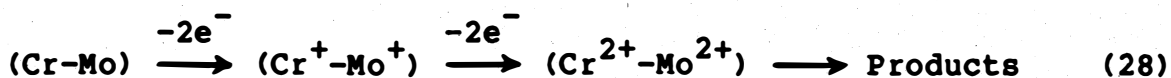


The shape of the primary anodic wave located at 0.94 volts versus  $\text{Ag}/\text{AgNO}_3$  and the fact that this wave was not coupled with a cathodic wave indicates a chemically irreversible process (FIGURE 9). The absence of the reduction wave on reversing the scan direction was indicative of a mechanism in which the (Cr-Mo) cation was removed through fast homogeneous chemical reaction following the electron-transfer step. [54] The electron-transfer consists of each metal center losing one electron when compared with that of ferrocene (EQUATION 28).

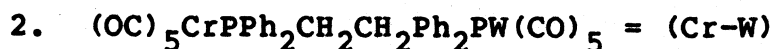
FIGURE 9. Voltammogram of  $5.18 \times 10^{-4}$  M  
 $(OC)_5CrPPh_2CH_2CH_2Ph_2PMo(CO)_5$   
in a 0.10 M TBAP-methylene  
chloride solution.  
(2.0 V/min.)



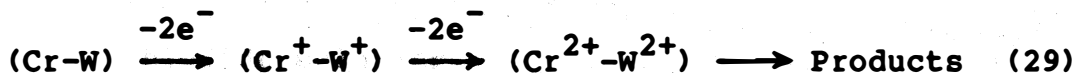




The second anodic peak located at +1.36 volts was characteristic of an adsorption peak similar to that of the (W-W) complex.



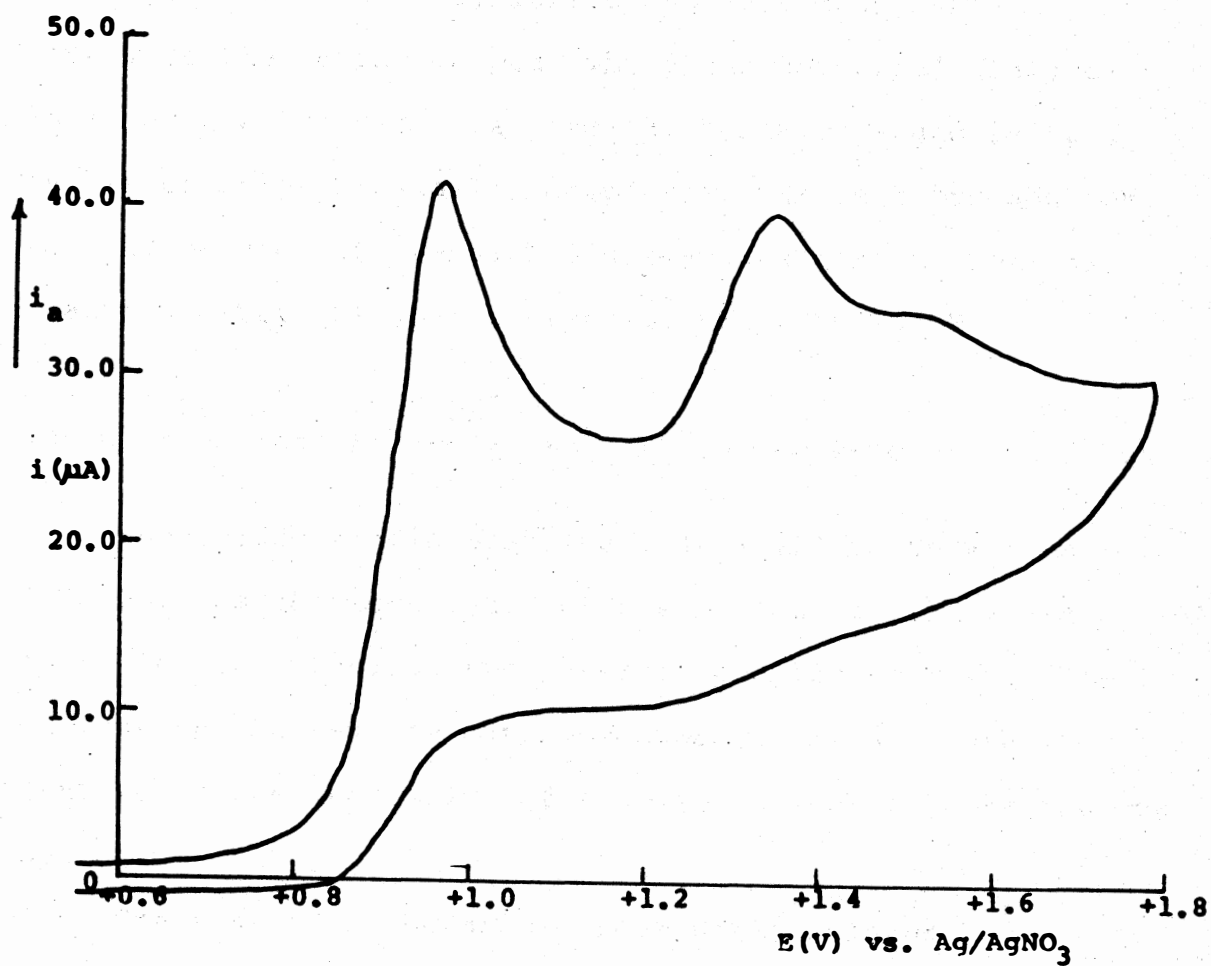
Irreversible behavior was also evident for the (Cr-W) complex because of the absence of the cathodic current on the reverse sweep (FIGURE 10). The anodic peak maximum which occurred at 0.96 volts versus Ag/AgNO<sub>3</sub> was characteristic of each metal center having a one-electron oxidation when compared to the peak current of ferrocene (EQUATION 29).

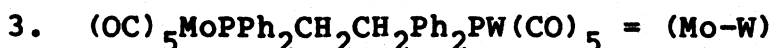


The second anodic peak was a stripping peak due to the oxidation of the film formed at the electrode surface. The location of the stripping peak, 1.36 volts versus Ag/AgNO<sub>3</sub>, was identical to the location of the (Cr-Mo) stripping peak.

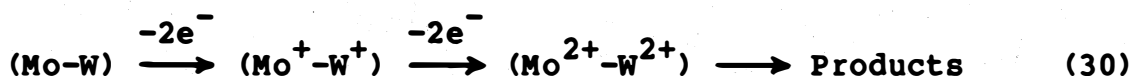
The (Cr-W) anodic peak maximum occurred .02 volts more positive than the anodic peak maximum for (Cr-Mo). This observation might have been expected because of what was discovered in the homometallic series. The (W-W) complex was found to be the most difficult to oxidize. Therefore, it made perfect sense to find (Cr-W) was harder to oxidize than (Cr-Mo).

FIGURE 10. Voltammogram of  $4.30 \times 10^{-4}$  M  
 $(OC)_5CrPPh_2CH_2CH_2Ph_2PW(CO)_5$   
in a 0.10 M TBAP-methylene  
chloride solution.  
(2.0 V/min.)





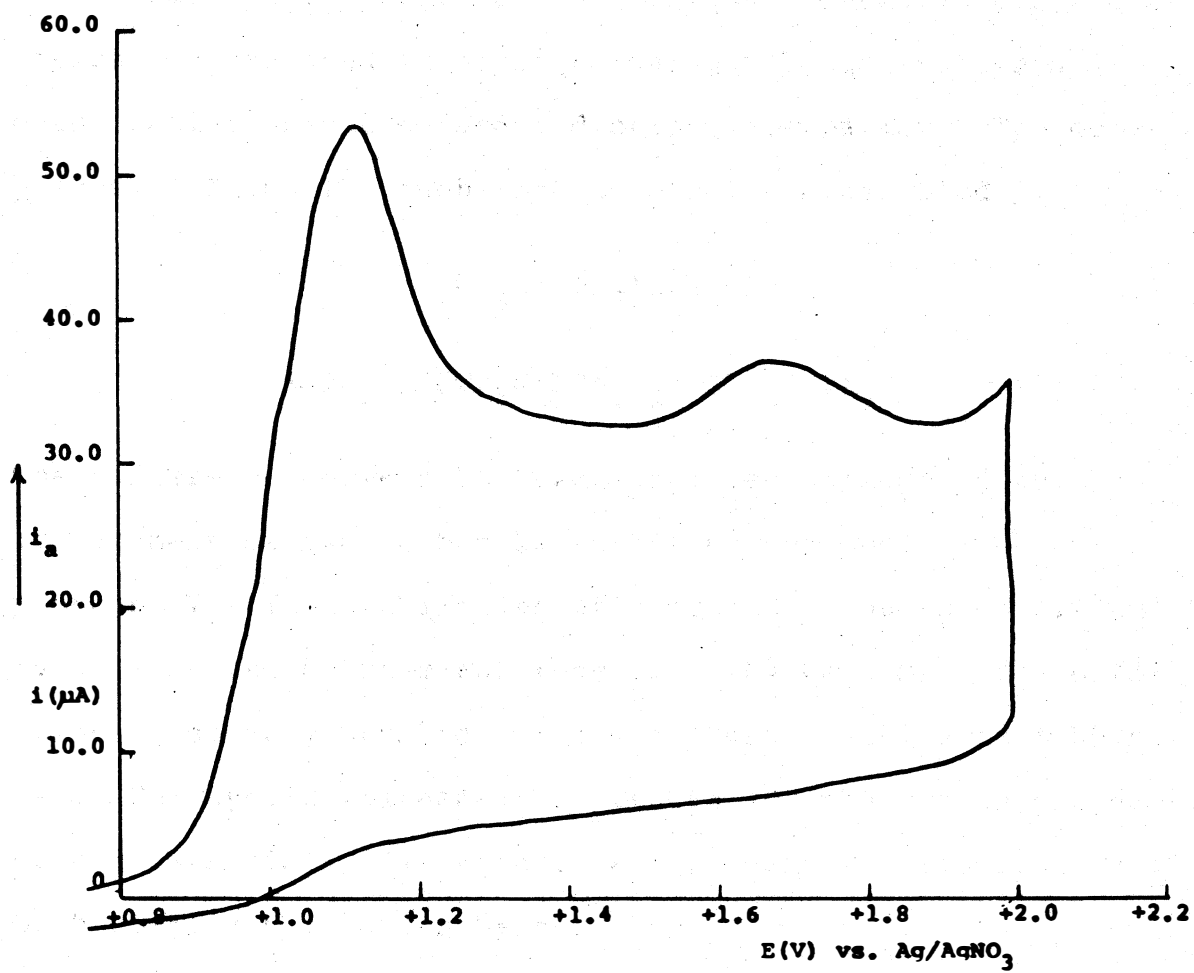
The cyclic voltammetric characteristics of the (Mo-W) species were very similar to the features of the other two heterobimetallic complexes in this series (FIGURE 11). A single anodic wave with the peak potential maximum at +1.05 volts versus Ag/AgNO<sub>3</sub> was found. The magnitude of the anodic peak current,  $i_{pa}$ , was equal to the loss of two electrons when compared to that of ferrocene. The anodic wave did not have a coupled cathodic peak which was a typical characteristic of the irreversible chemical behavior found in this series of heterobimetallic complexes. The best explanation for the absence of the cathodic peak was a fast chemical reaction after the charge transfer step (EQUATION 30).



The second anodic peak found at +1.64 volts versus Ag/AgNO<sub>3</sub> was characteristic of the stripping peak as was found for the previous two heterobimetallic species. The current on the reverse cathodic sweep decayed to the base line which was indicative of film formation on the electrode surface.

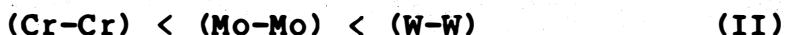
The fact that the anodic peak potential for the (Mo-W) complex was .09 volts versus Ag/AgNO<sub>3</sub> more positive than the (Cr-W) species and .11 volts more positive than the (Cr-Mo) complex explains the difficulty of oxidation for the heterobimetallic series (SCHEME I).

FIGURE 11. Voltammogram of  $4.93 \times 10^{-4}$  M  
 $(OC)_5MoPPh_2CH_2CH_2Ph_2PW(CO)_5$   
in a 0.10 M TBAP-methylene  
chloride solution.  
(10.0 V/min.)





This finding for the heterobimetallic series was in complete agreement with the difficulty of oxidation found for the homobimetallic series (SCHEME II).

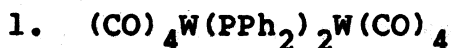


### C. PHOSPHIDO-BRIDGED TUNGSTEN CARBONYLS

A pair of phosphido bridged tungsten metal carbonyl complexes was examined in order to gain both qualitative and quantitative oxidation and reduction information. The complexes, III and IV, each contain a metal-metal bond.



The difference between the two complexes depends on the replacement of two carbonyls in III by two phosphines to produce IV. The stabilities of oxidized products of III and IV as measured by chemical reversibility were markedly different presumably because IV is much more electron rich than III. The cyclic voltammetric results for the two complexes were substantially different. A more detailed description of both complexes is given below.

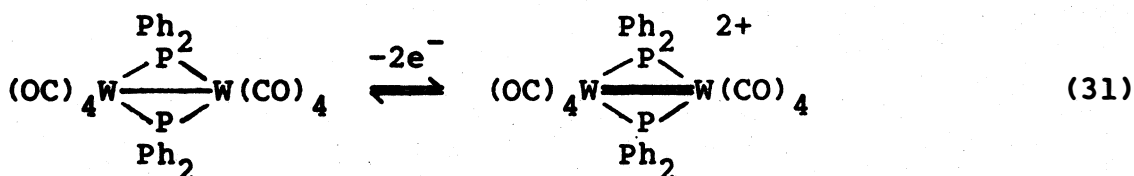


The first anodic peak showed a well-defined current maximum at +0.750 volts and was consistent with a one- elec-



tron oxidation of each metal center when compared to that of ferrocene. On reversal of the sweep, a coupled cathodic peak was found at +0.68 volts. The magnitude of the cathodic peak current,  $i_{pc}$ , was also found to be consistent with two one-electron transfers (FIGURE 12). Examination of the separation of the peak potentials,  $\Delta E_p$ , for the first wave showed values characteristic of a quasi-reversible system.

[55] The difference between the anodic peak,  $E_{pa}$ , and the cathodic peak,  $E_{pc}$ , was equal to 73 mV. For a Nernstian or reversible response the value would have been 59 mV. The ratio of the anodic peak current to the cathodic peak current was equal to 0.98, an indication that the oxidation product was stable over the time period of the measurement. [56] This anodic and cathodic couple corresponds to the mechanism for the tungsten-tungsten oxidation being a simple process uncomplicated by coupled chemical reactions. Formally it corresponds to converting the metal-metal single bond into a metal-metal double bond (EQUATION 31).



When the single sweep cyclic voltammogram of the tungsten-tungsten complex was carried out to +1.02 volts a second anodic peak maximum was discovered (FIGURE 13). There was no coupled cathodic wave found on the reverse scan. Such

FIGURE 12. Voltammogram (first peak) of  $3.68 \times 10^{-4}$  M  
 $(OC)_4W(PPh_2)_2W(CO)_4$  in a 0.10 M TBAP-  
methylene chloride solution (2.0 V/min.).

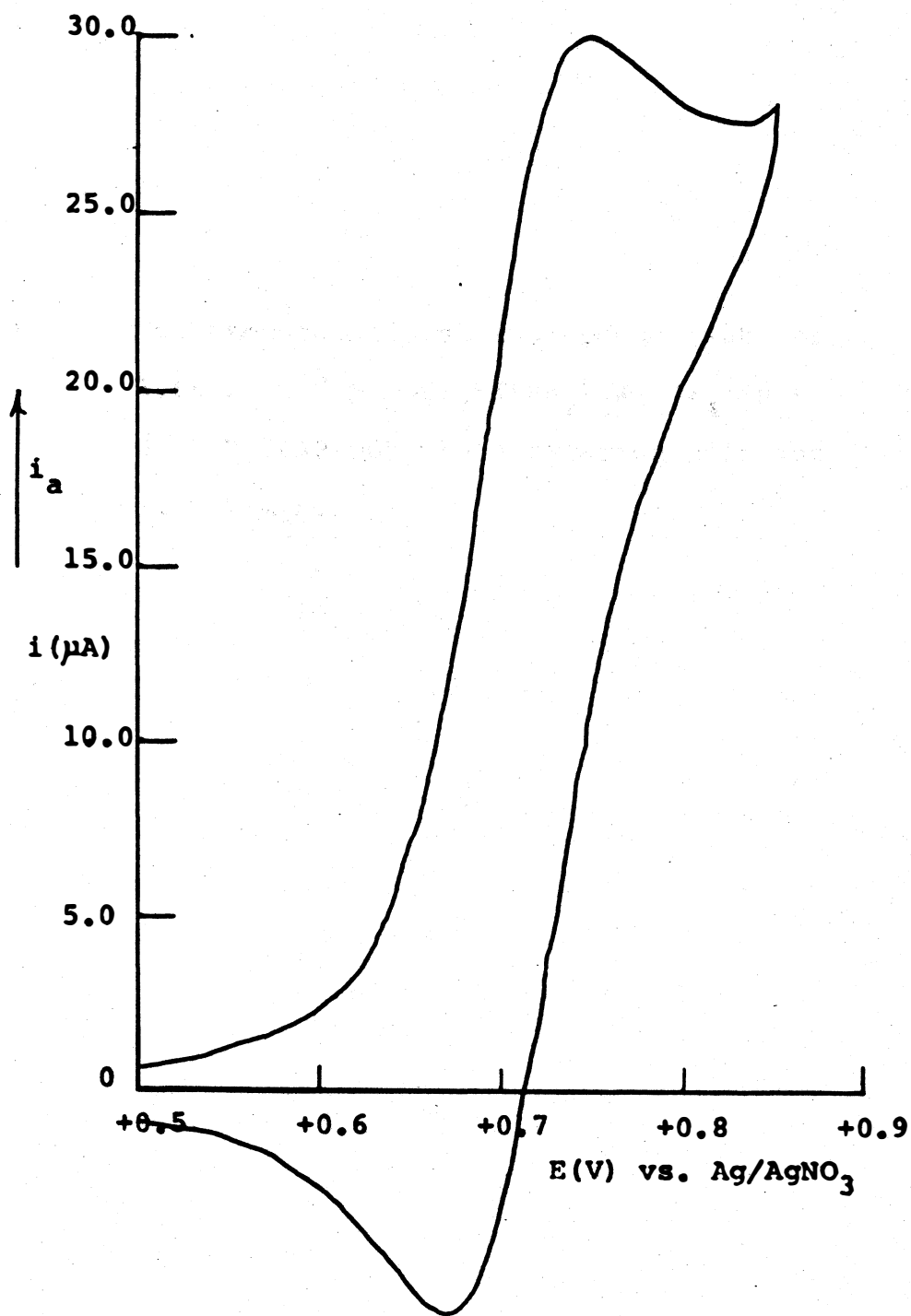
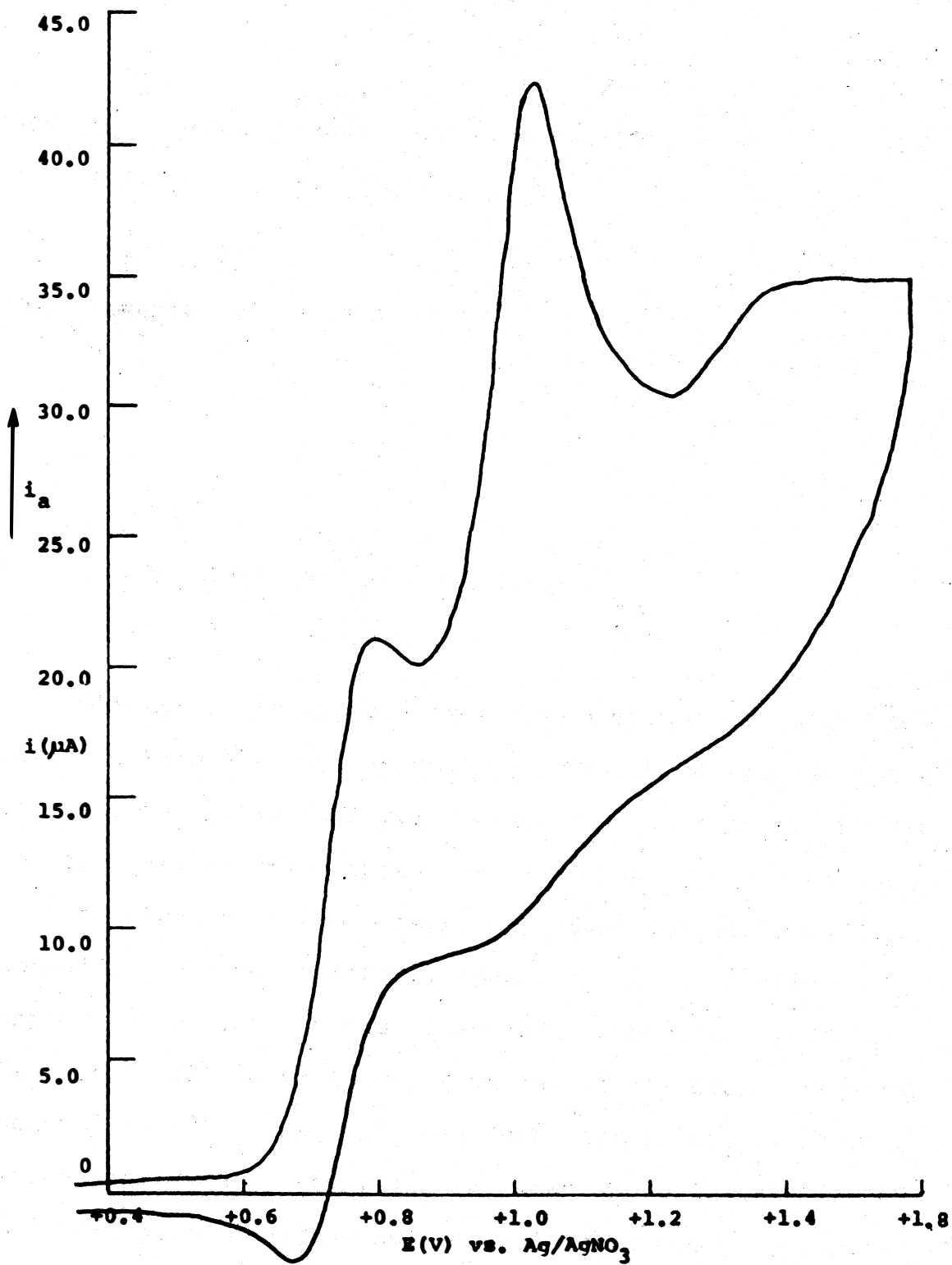
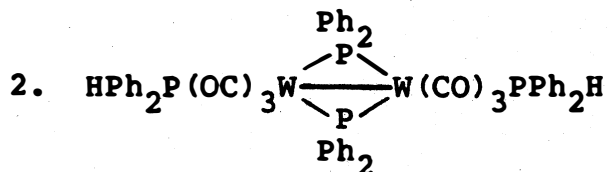
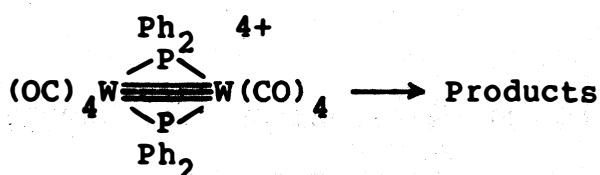
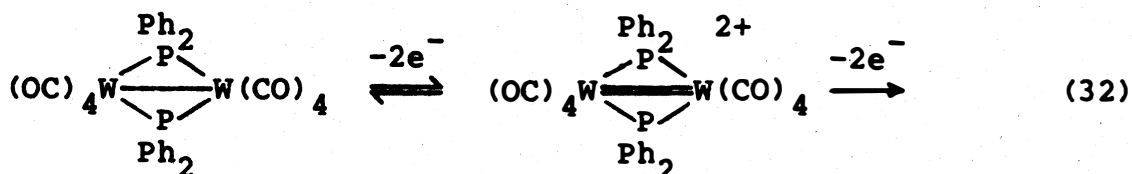


FIGURE 13. Voltammogram (first and second peak) of  $3.68 \times 10^{-4}$  M  $(OC)_4W(PPh_2)_2W(CO)_4$  in a 0.10 M TBAP-methylene chloride solution (1.0 V/min.).



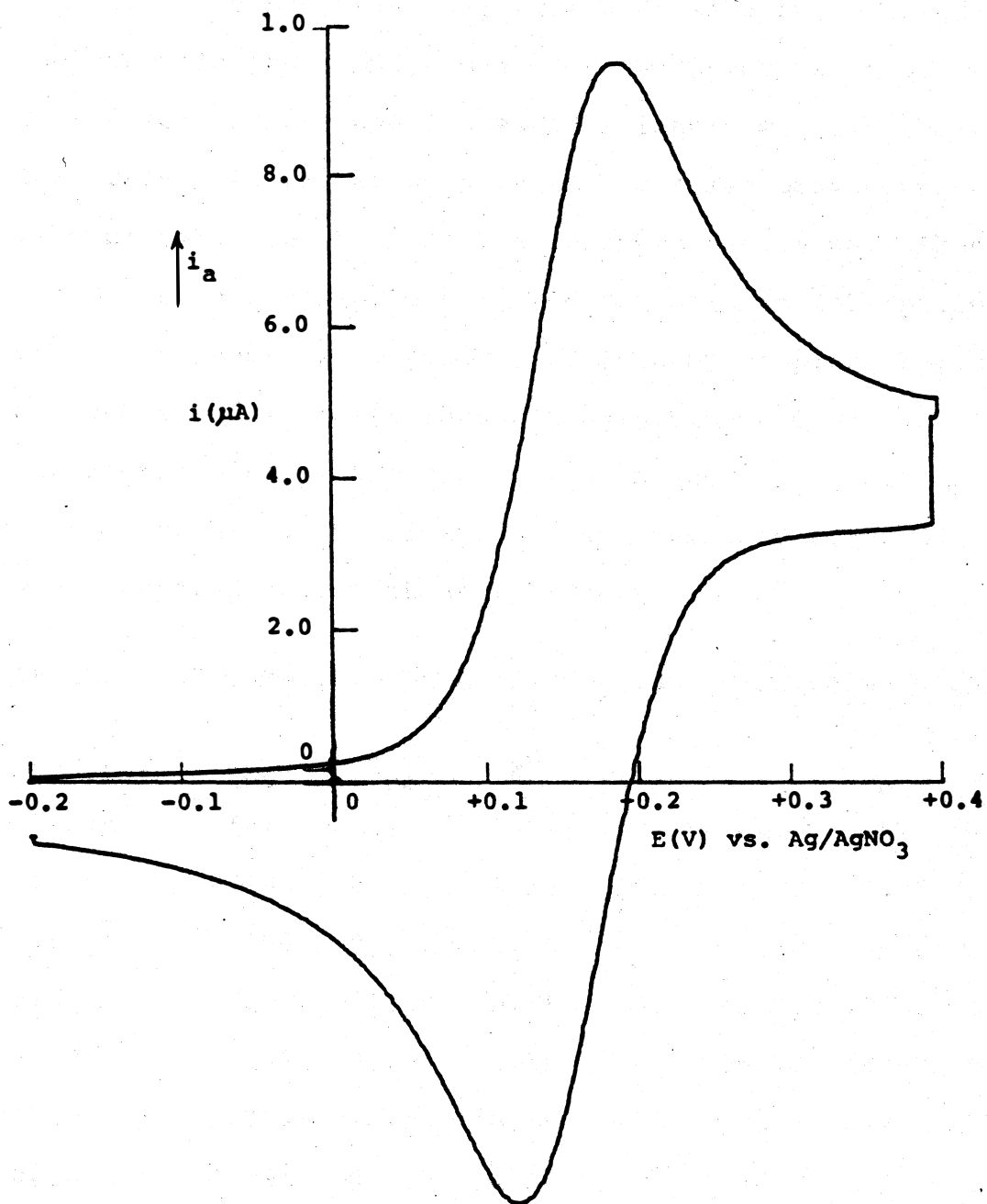
behavior suggests that the second two-electron transfer was electrochemically irreversible. The absence of the reverse electron-transfer step derives from the rapid decomposition of the cation (EQUATION 32).



The cyclic voltammetry for this tungsten-tungsten complex exhibits the most Nernstian (reversible) behavior of all the group VI metal carbonyl complexes in this study (FIGURE). For this reason this complex was examined in the most detail.

A solution of the phosphido-bridged complexes in  $\text{CH}_2\text{Cl}_2$ , containing 0.1 molar (TBAP), when examined by cyclic voltammetry at a platinum disc electrode, showed an oxidation peak at +0.182 volts and on reversal of the scan a reduction peak at +0.120 volts. The reversibility of the first wave was established by reversing the scan approximately 120 mV past the first anodic peak. Cyclic voltammetry data were

FIGURE 14. Voltammogram (first peak) of  $3.22 \times 10^{-4}$  M  
 $\text{HPh}_2\text{P}(\text{OC})_3\text{W}(\text{PPh}_2)_2\text{W}(\text{CO})_3\text{PPh}_2\text{H}$  in a 0.10 M  
TBAP-methylene chloride solution  
(2.0 V/min.).





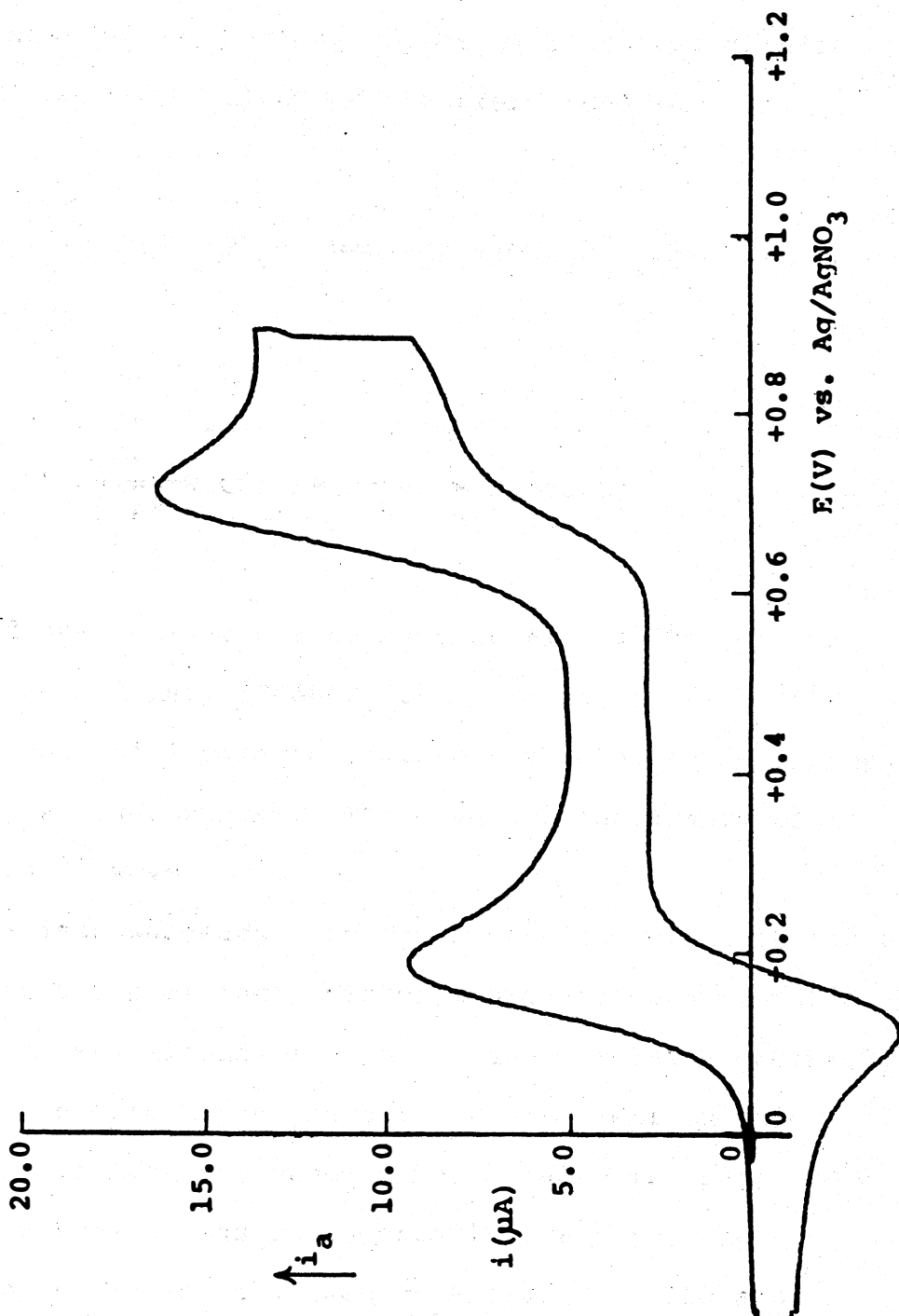
collected over the range of scan rates 1.0 to 50.0 volts/minute (TABLE 5). The ratio of the anodic-to-cathodic peak current was constant and near one. An inspection of the details of the sweep dependence reveals that the current function,  $i_p/v^{1/2}$ , was constant, in accordance with diffusion control. The potential separation between the coupled anodic and cathodic peaks,  $\Delta E_p$ , was close to 60 mV for sweep rates of 1.0 volt/minute and increased slightly with increase in scan rate. At faster scan rates increased peak separations were probably due to solution resistance effects. These properties are consistent with electron-transfers processes which are reversible or uncomplicated by coupled chemical reactions and indicate that the oxidation product was stable during the time of the sweep. The number of electrons involved in the first oxidation was determined to be about one when compared with that of ferrocene.

TABLE 5. VOLTAMMETRIC DATA of  $\text{HPh}_2\text{P}(\text{OC})_3\text{W}(\text{Ph}_2\text{P})_2\text{W}(\text{CO})_3\text{PPh}_2\text{H}$

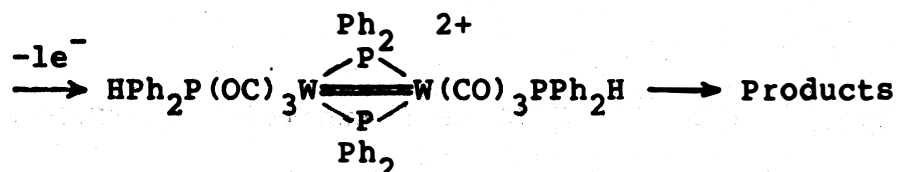
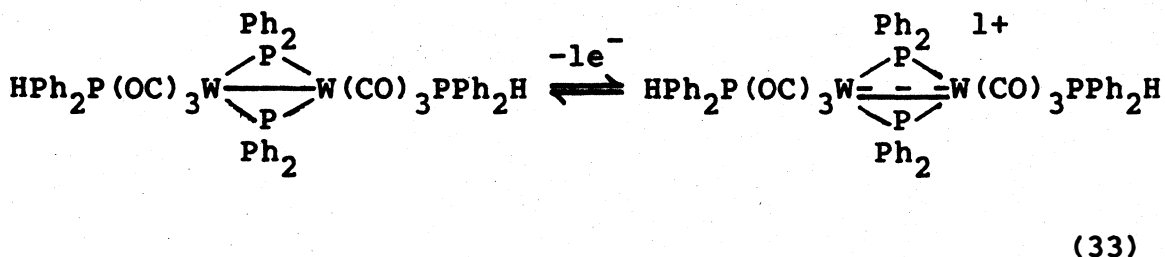
SCAN RATE (V/min.)	$E_{pa}$ (V)	$E_{pc}$ (V)	$E^0$ (V)	$\Delta E_p$ (mV)	$i_{pa}$ ( $\mu\text{A}$ )	$i_{pc}$ ( $\mu\text{A}$ )	$i_{pa}/i_{pc}$ ---
1.0	0.182	0.120	0.15	62	5.71	5.67	1.01
2.0	0.190	0.122	0.16	68	7.80	7.76	1.01
5.0	0.196	0.120	0.16	76	12.11	12.01	1.01
10.0	0.198	0.114	0.16	84	16.73	16.93	0.99
20.0	0.215	0.115	0.16	100	26	24	1.08
50.0	0.225	0.100	0.16	125	38	34	1.12

A second anodic peak (FIGURE 15 ) showing a well defined

FIGURE 15. Voltammogram (first and second peak) of  
 $3.22 \times 10^{-4}$  M  $\text{HPh}_2\text{P}(\text{OC})_3\text{W}(\text{PPh}_2)_2\text{W}(\text{CO})_3\text{PPh}_2\text{H}$   
in a 0.10 M TBAP-methylene chloride solution  
(2.0 V/min.).



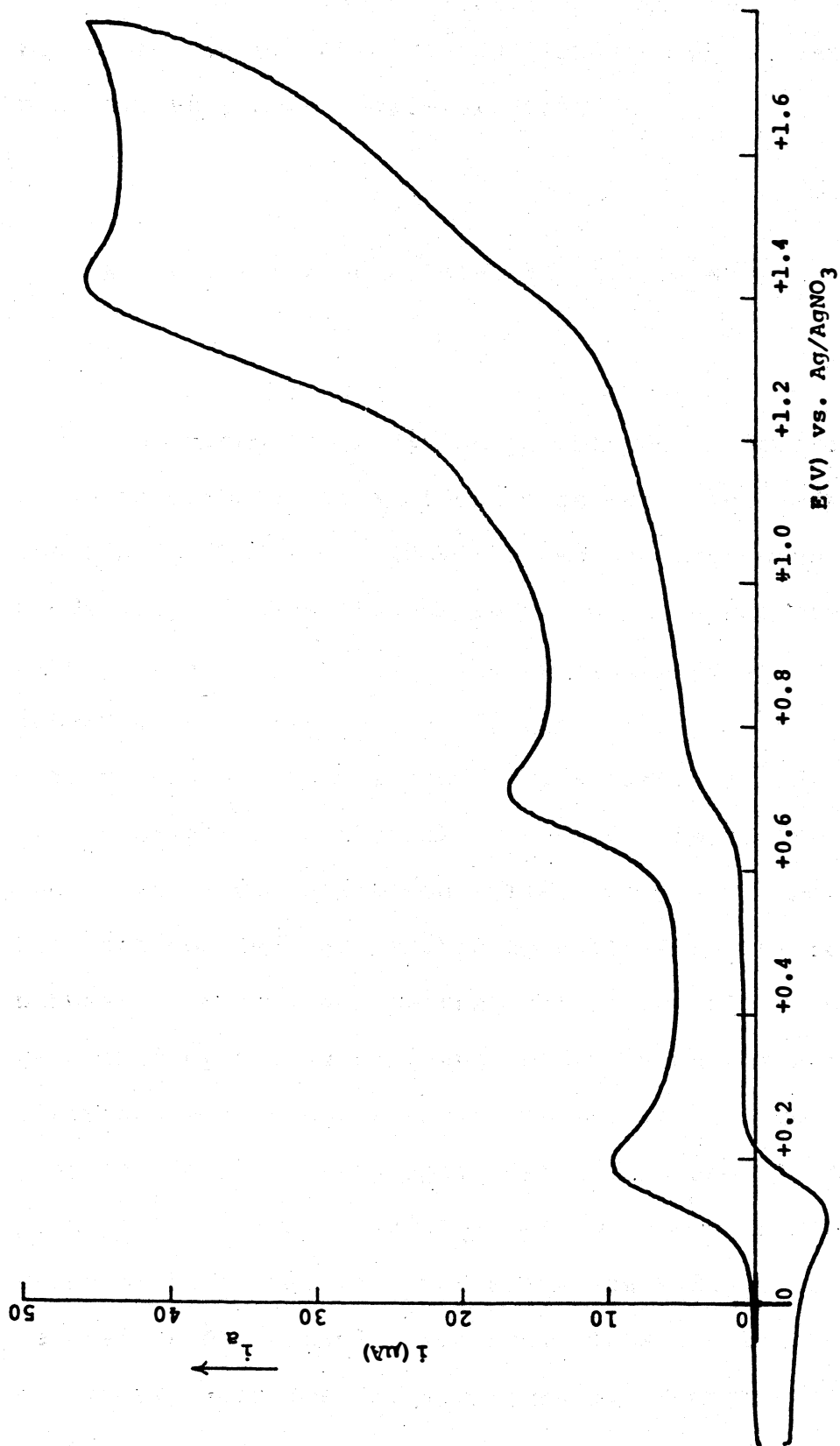
current maximum at +0.72 volts was found but did not possess a coupled cathodic peak on the reverse scan. Such behavior suggests that the second oxidation step, consisting of a one-electron transfer, can best be explained by a fast chemical reaction following the electron transfer (EQUATION 33).



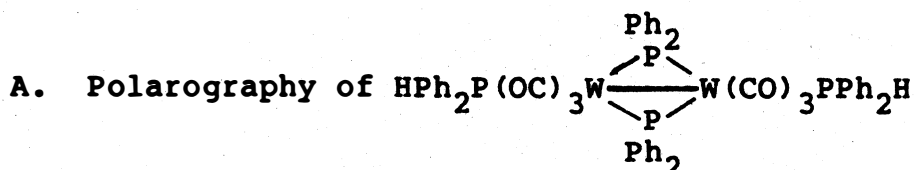
A third anodic wave was present at +1.4 volts but was not a well-defined peak (FIGURE 16). The magnitude of the peak current was difficult to compare with that of ferrocene because of the rounded peak. There was no appearance of a coupled cathodic wave.

A comparison was made between the anodic peak potentials for the first waves of these two phosphido-bridged tungsten carbonyls. As was already mentioned, the oxidation potential was found to be strongly dependent on the number and the nature of the ligands surrounding the metal. The magnitude of the peak potential was substantially lower for the tungsten complex having the two  $\text{HPh}_2\text{P}$  ligands. The anodic peak potential was found to be 0.56 volts less positive than the tungsten complex without the two  $\text{HPh}_2\text{P}$  ligands. The substitution of one carbonyl ligand on each metal by  $\text{HPh}_2\text{P}$

FIGURE 16. Voltammogram (1<sup>st</sup>, 2<sup>nd</sup> and 3<sup>rd</sup> peak) of  
 $3.22 \times 10^{-4}$  M  $\text{HPh}_2\text{P}(\text{OC})_3\text{W}(\text{PPh}_2)_2\text{W}(\text{CO})_3\text{PPh}_2\text{H}$   
in a 0.10 M TBAP-methylene chloride solution  
(2.0 V/min.).



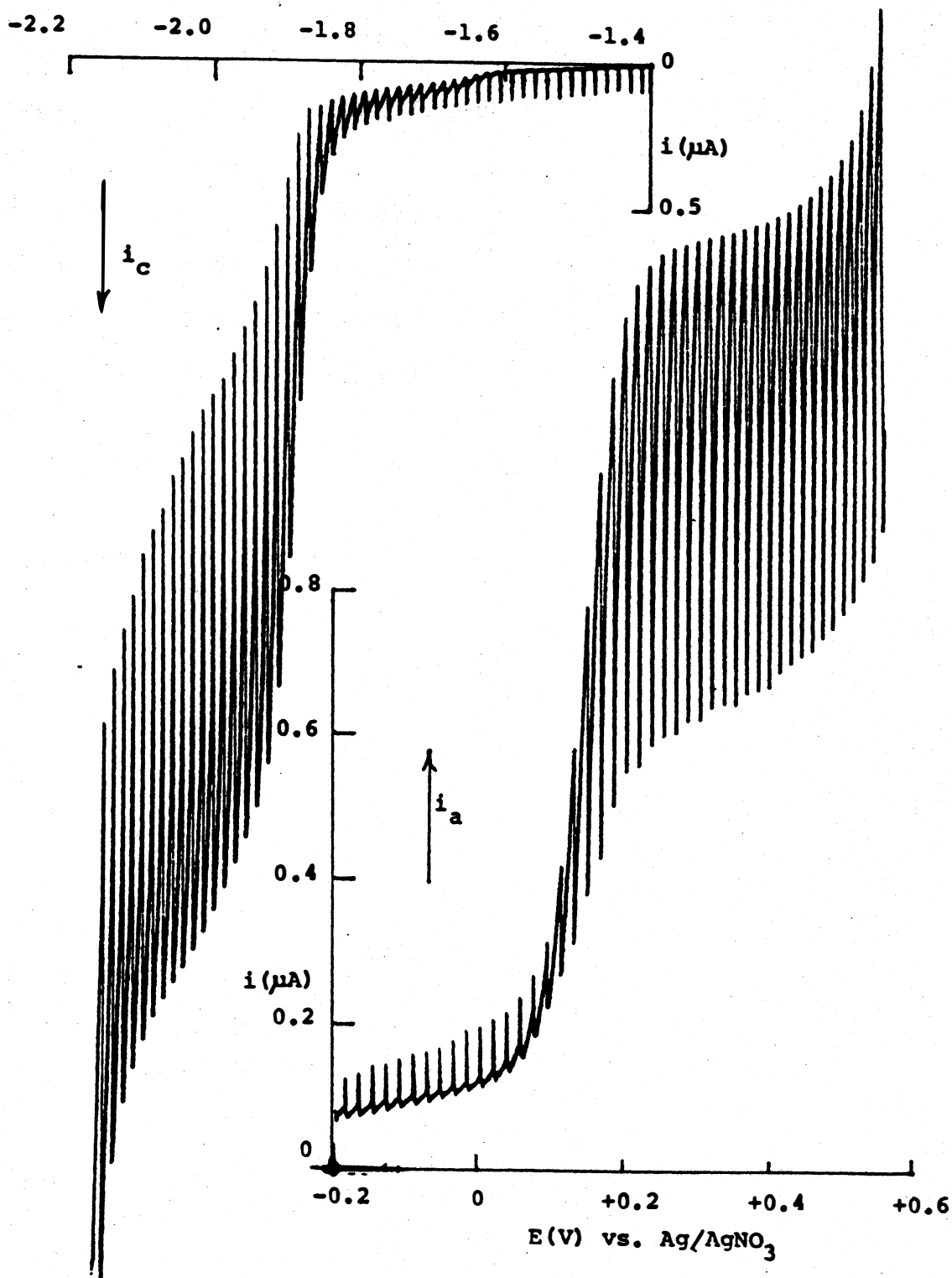
causes a change in the electrochemistry of the two systems. As the carbonyl ligands were replaced by the  $\text{HPh}_2\text{P}$  ligands, which are poorer  $\pi$ -acids, the tungsten metal centers became progressively more easily oxidized.



Polarographic oxidation of the phosphido-bridged tungsten carbonyl at a dropping mercury electrode in  $\text{CH}_2\text{Cl}_2$  containing 0.1 molar (TBAP) showed one wave when scanned anodically (FIGURE 17). A reduction wave was observed, but since the wave occurred close to discharge (-2.2 volts), interpretation was very difficult. The wave height or current plateau of the anodic wave varied as the square root of the height of the dropping mercury electrode,  $(h)^{1/2}$ , indicating a diffusion-controlled process. Since the tungsten complex was limited by diffusion, the relationship between potential and current for a reversible polarogram as described by Meites was used to determine the number of electrons and to check the reversibility of the electron process. [57] Polarographic data are found in TABLE 6 and a plot of  $E_{\text{DME}}$  versus  $\log[(i_d - i)/i]$  is shown in FIGURE 18. A slope of 52 mV was obtained which was indicative of a reversible one electron process. This was also observed in the cyclic voltammetric experiments. From the Y-intercept a half-wave potential of +0.14 volts was found, which was in

FIGURE 17. Polarogram of  $3.22 \times 10^{-4}$  M  
 $\text{HPh}_2\text{P}(\text{OC})_3\text{W}(\text{PPh}_2)_2\text{W}(\text{CO})_3\text{PPh}_2\text{H}$   
in a 0.10 M TBAP-methylene  
chloride solution.





agreement with the graphically determined  $E_{1/2}$  value and the  $E_{1/2}$  value determined by cyclic voltammetry.

TABLE 6. POLAROGRAPHIC DATA of  $\text{HPh}_2\text{P}(\text{OC})_3\text{W}(\text{Ph}_2\text{P})_2\text{W}(\text{CO})_3\text{PPh}_2\text{H}$

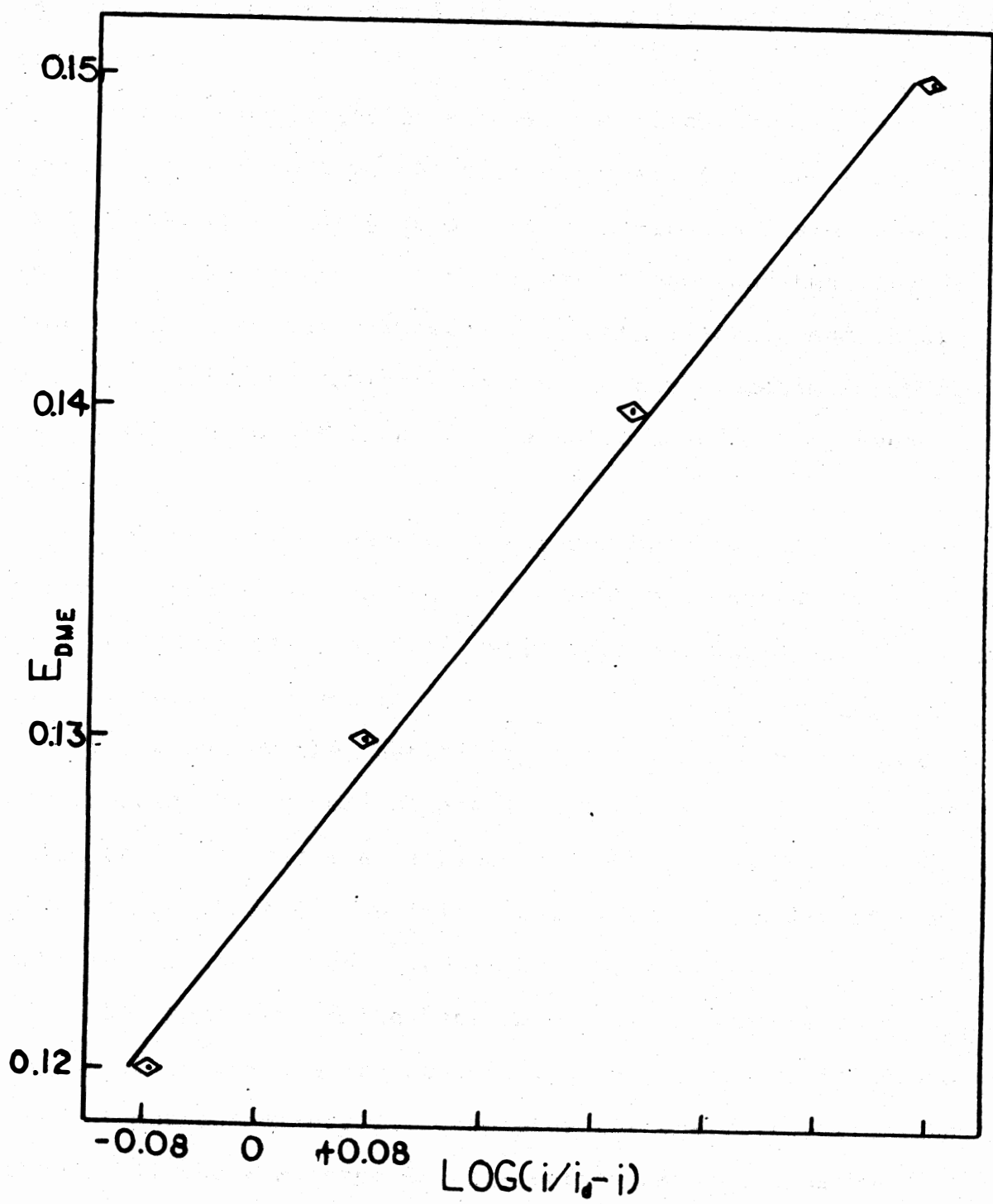
$h(\text{corr}) = 53.2 \text{ cm}$        $i_d = 1.16 \mu\text{A}$

$E_{\text{DME}}$ (V)	$i$ ( $\mu\text{A}$ )	$\text{LOG}(i/i_d - i)$
0.120	0.53	-0.075
0.130	0.63	+0.075
0.140	0.75	+0.262
0.150	0.87	+0.477

FIGURE 18. Plot of EQUATION 5. Reversibility, n and

$E_{1/2}$  determination of

$\text{HPh}_2\text{P}(\text{OC})_3\text{W}(\text{Ph}_2\text{P})_2\text{W}(\text{CO})_3\text{PPh}_2\text{H}.$



#### IV. CONCLUSIONS

Electrochemical data in this study provide strong evidence for the existence of individual 17-electron metal centers for both the homobimetallic and the heterobimetallic complexes.

In the homobimetallic series, the chromium-chromium species appears to have the most stability for the first oxidation step as was shown by the quasi-reversible behavior. The first oxidation step for molybdenum and tungsten, show that the 17-electron complexes were both reactive and unstable. A following chemical reaction of the oxidation product was evident from the lack of a cathodic peak on the reverse scan.

A second oxidation step was found only for the chromium-chromium complex, which leads to unstable products. The final products have not been determined but would aid in the overall reaction scheme.

The trend in the instability of the oxidized products for homobimetallic series parallels both the difficulty with which the complexes are oxidized,  $(\text{Cr-Cr}) < (\text{Mo-Mo}) < (\text{W-W})$ , and the magnitude of the first ionization potentials of the individual gaseous metal atoms:  $\text{Cr} < \text{Mo} < \text{W}$ .

The chemistry of the heterobimetallic complexes, as indicated by the electrochemistry, is essentially similar to that of the homobimetallic complexes for the first oxidation step. All the complexes in this series have no apparent stability. After the first oxidation the complexes either

disproportionate or rearrange to give unknown products. In either case it would not be surprising to find that if chemical oxidation were carried out, isolation would be difficult. The attempt to oxidize a single metal center of a heterobimetallic complex while the other metal center remained neutral was unsuccessful.

It is possible that the product decomposition reaction might be sufficiently dependent a low temperature electrochemistry experiment might reveal stable oxidized products. The reversibility of the oxidized products could be seen since the follow-up chemical reaction would be quenched.

The instability of all these complexes is probably associated with the extreme reactivity of the oxidized species. The  $E^0$  values for the redox couples are all very positive. The electrochemical or chemical oxidation and subsequent isolation seems to be rather difficult due to these very positive potentials. For example, a sufficiently powerful oxidant would have to be strong enough to produce the stable Cr(I) species. However, complications could arise if the oxidant is too strong, and the Cr(II) species is formed, which is only 0.3 volts more positive than the Cr(I). This shows the need for being very selective when oxidizing this complex and why it is advantageous to use electrochemical synthetic methods.

The considerable stability of the two phosphido-bridged complexes arises from the metal-metal bond and the presence of two bridging ligands. The ease with which these complexes can be oxidized suggests the possibility of isolating the

oxidized product as a salt using a counter ion. For complex (IV) the electrosynthesis may be more selective since the peak separations for the first reversible oxidation peak and the second irreversible oxidation peak is 0.5 volts.

This fundamental electrochemical study such has revealed the detailed nature of the charge-transfer steps involved in these novel group VI transition metal carbonyls. An understanding of the probable mechanisms of oxidation of these complexes obviously has important synthetic implications and work in this area should be followed up. In particular, product analysis of the 17-electron species by electron spin resonance and the 18-electron species by  $^{31}\text{P}$  NMR would give a more complete picture of the redox properties of these carbonyl complexes.

## LITERATURE CITED

1. Headridge, J.B., "Electrochemical Techniques for Inorganic Chemists," Academic Press, New York, (1969).
2. Albers, M.O., Coville, N.J., Coord. Chem. Reviews, 53(1984) pp. 227-259.
3. Bard, A.J., Faulkner, L.R., "Electrochemical Methods," John Wiley and Sons, New York, (1980), p. 19.
4. Bard, A.J., Faulkner, L.R., Ibid p. 27.
5. Adams, R.N., "Electrochemistry at Solid Electrodes," Marcel Dekker, New York, (1969), p. 119.
6. Adams, R.N., Ibid p. 70.
7. Adams, R.N., Ibid p. 116.
8. Marcus, R.A., J. Chem. Phys., 43, 679 (1965).
9. Lukehart, C.M., "Fundamental Transition Metal Organometallic Chemistry", Brooks/Cole, California (1985) pp. 398-405.
10. Hershberger, J.W., Klinger, R.J., Kochi, J.K., J. Am. Chem. Soc., (1982), 104, pp. 3034-3043.
11. Bond, A.M., Colton, R., Jackowski, J.J., Inor. Chem., Vol. 14, No. 2, (1975), pp. 274-277.
12. Bond, A.M., Colton, R., Kevekordes, J.E., Ibid, Vol. 25, No. 6, (1986), pp. 749-756.
13. Hershberger, J.W., p. 3037.
14. Dessy, R.E., Rheingold, A.L., Howard, G.D., Organometallic Electrochemistry, 94:3, Feb. 9, 1972.
15. Wojcicki, A., Inorganica Chimica Acta, 100 (1985) 125-133.
16. Therien, M.J., Ching-Long Ni, Anson, F.C., Osteryoung, J.G., Trogler, W.C., J. Am. Chem. Soc., 108, 4037-4042 (1986).
17. Coutagne, D., Bull. De LA Soc. Chim. De France (1971) No. 5, pp. 1940-1946.



18. Weissberger, Technique of Organic Chemistry, Vol. VII, organic solvents, Interscience Publishers, London, 1955, p. 192.
19. Bard, A.J., p. 148.
20. Keiter, R.L., Kaiser, S.L., Hansen, N.P., Bradack, J.W., Cary, L.W., Inorg. Chem, 1981, 20, 283.
21. Keiter, R.L., Keiter, E.A., Mittelberg, K.N., Martin, S.M., Meyers, V.N., Unpublished results.
22. Meites, L., "Polarographic Techniques," 2nd., Interscience, New York, 1965, p. 103.
23. Meites, L., p. 213.
24. Bard, A.J., pp. 699-702.
25. Willard, H.H., Merritt, L.L., Dean, J.A., Settle, F.A., "Instrumental Methods of Analysis", D.VanNostrand, New York, (1981) pp. 634-638.
26. Mann, C.K., Electroanal. Chem. 1969, 3, 57-134.
27. Hershberger, J.W., p. 3036.
28. Bond, A.M., Colton, R., McGregor, K., Inorg. Chem., 1986, 25, 2378-2384.
29. Koepp, H.M., Wendt, H., Strehlow, H.Z., Elektrochem, 1960, 64, 483-491.
30. Bauer, D; Beck, J.P., Bull. Soc. Chim. Fr., 1973, 1252-1259.
31. Alexander, R., Parker, A.J., Sharp, S.H., Waghorne, W.E., J. Am. Soc., 1972, 94, 1148-1158.
32. Nicholson, R.S., Shain, I., Anal. Chem. 36, 706 (1964).
33. Delahay, P., "New Instrumental Methods in Electrochemistry", Interscience, New York, 1954, p. 119.
34. Bard, A.J., P. 148.
35. Delahay, P., p. 64.
36. Meites, L., p. 218.
37. Nicholson, R.S., Anal. Chem., Vol. 37, No. 11, 1965, 1351-1356.

38. Bagchi, R.N., Bond, A.M., Brain, G., Colton, R.,  
Henderson, T.L., Kevekordes, J.E., Organometallics  
1984,3,4.
39. Reinmuth, W.H., Anal Chem, 1960,32,1891.
40. Bond, A.M., Colton, R., Jackowski, J.J., Inor. Chem.,  
14, No. 2, (1975), p. 274-277.
41. Nicholson, R.S., Shain, I., Anal. Chem., 36, 706 (1964).
42. Cotton, F.A., Wilkinson, G., "Advanced Inorganic  
Chemistry", 4th ed., Wiley-Interscience, New York,  
1980, p. 1070.
43. Huheey, J.E., "Inorganic Chemistry", 3rd ed., Harper-  
Row, New York, 1983, p. 365-367.
44. Hershberger, J.W., Klingler, R.J., Kochi, J.K., J.Am.  
Chem. Soc., 1982, 104, p. 30-35.
45. IBID., p. 3040.
46. Bond, A.M., Colton, R., Jackowski, J.J., Inor. Chem.,  
Vol. 14, No. 2, 1975.
47. Keiter, R.L., Kaiser, S.L., Hansen, N.P., Brodack, J.W.,  
Carg, L.W., Inorg. Chem., 20, 1981, p. 283.
48. See reference 44.
49. Huheey, J.E., p. 147-148.
50. See reference 44.
51. See reference 46.
52. Adams, R.M., p. 125, p. 191.
53. Shain, R.S., Anal. Chem. 39, 1535 (1967).
54. Tetsuo, O., Attila, Y., Kuwana, T., J. Am. Soc. 91, 3994  
(1969).
55. Nicholson, R.S., Shain, I., Anal. Chem. 37, 178 (1965).
56. Nicholson, R.S., Shain, I., Anal. Chem. 37, 190 (1965).
57. Meites, L. p. 218.

## VITA

**DWAYNE EDWARD COOPER**

### Birth Place

**Dexter, Missouri  
March 16, 1959**

### Education

**Maine North High School  
DesPlaines, Illinois  
1973-1977**

**Eastern Illinois University  
Charleston, Illinois  
1977-1982 B.S. Chemistry**

**Illinois State Water Survey  
Champaign, Illinois  
1982-1984 Research Chemist**

**Eastern Illinois University  
Charleston, Illinois  
1984-1986 M.S. Chemistry**